Nagaraj Vinayagam Govindaraj

Light-weight materials produced by accumulative roll bonding

Thesis for the degree of Philosophiae Doctor

Trondheim, April 2013

Norwegian University of Science and Technology
Faculty of Natural Sciences and Technology
Department of Materials Science and Engineering

NTNU – Trondheim
Norwegian University of
Science and Technology

NTNU
Norwegian University of Science and Technology

Thesis for the degree of Philosophiae Doctor

Faculty of Natural Sciences and Technology
Department of Materials Science and Engineering

ISBN 978-82-471-4328-5 (printed ver.)
ISBN 978-82-471-4329-2 (electronic ver.)
ISSN 1503-8181

Doctoral theses at NTNU, 2013:114

Printed by NTNU-trykk

To

the sitcom “Friends”

&

my parents

PREFACE

This work has been carried out at the Department of Materials Science and Engineering, Norwegian University of Science and Technology (NTNU) over a three year period from Nov 2009 to Nov 2012. This work is a part of the Innovation in light metals processing and manufacture involving the use of severe plastic deformation for nano-structuring, mechanical alloying and interfacial bonding (Improvement) project under the Strategic University Program at NTNU. The main objective of this project is to fully explore and document the potential of using severe plastic deformation (SPD) for nano-structuring, mechanical alloying and interfacial bonding as a basis for future process innovation and material and product development within the Norwegian light metals industry. In the present work, the focus has been on implementing, developing and benchmarking the ARB process for fabrication of multilayered metal composites to primarily produce new light- weight materials for structural applications. Three different journal publications have been prepared during the course of the work.

ARTICLE 1

Nagaraj Vinayagam Govindaraj, Steinar Lauvdal, Bjørn Holmedal

Tensile Bond strength of cold roll bonded aluminium sheets

Published in Journal of Materials Processing Technology

ARTICLE 2

Nagaraj Vinayagam Govindaraj, Ruben Bjørge, Bjørn Holmedal

Hardening on annealing in cold rolled AA3103 strips

Submitted to Metallurgical and Materials Transactions A

ARTICLE 3

Nagaraj Vinayagam Govindaraj, Jan Gaute Frydendahl, Bjørn Holmedal

Layer continuity in accumulative roll bonding of dissimilar material combinations

Under review in Materials and Design

These three articles constitute the second part of the thesis. The articles are independent of each other and are presented in the sequence in which the work progressed.

ACKNOWLEDGEMENTS

Any accomplishment requires the efforts of many people and this work is not different. This work was carried out under the supervision of Prof. Bjørn Holmedal and Prof Knut Marthinsen at the Department of Materials Science and Engineering. I would like to express my sincere gratitude to my main supervisor Prof. Bjørn Holmedal for his constant encouragement, scientific and professional discussions and constructive guidance during the last three years. I also wish to express my gratitude to my co-supervisor Prof. Knut Marthinsen for his timely help and support at critical times.

This work has been financed by the Research Council of Norway under the Strategic University Program project Improvement. AA3103 material used in this investigation was provided by Norsk Hydro AS. I also would like to acknowledge Loctite Norway AS for providing the surface preparation and gluing kit used in the tensile bond strength measurement experiments.

The technical personnel at the Department of Materials Science and Engineering deserve a huge acknowledgement. Engineers Pål Christian Skaret, Pål Ola Ulseth and Torild Krogstad have always been of timely help with sample preparation and testing. I also wish to thank senior engineer Yingda Yu for providing training at the electron microscopy laboratory. The team of technicians at the precision machining workshop working with Harald Snekvik deserves special thanks. I wish to record my sincere gratitude to higher executive officers Hilde Martinsen Nordø, Elin Synnøve Isaksen Kaasen at the Department of Materials Science and

Engineering and adviser Marit Svendsen from Human Resources division for being very helpful with the administrative work especially during the extension period.

I am grateful to the two master students I co-supervised during this period. Steinar Lauvdal had been very supportive in the roll bonding and tensile bond strength experiments. My sincere thanks are also due to Jan Gaute Frydendahl for his help with most of the accumulative roll bonding experiments in the similar and dissimilar material combinations.

I record my deep sense of gratitude to my collaborators, friends and colleagues in my research group who have helped me a lot during different stages of this work :- Prof. Henry Sigvart Valberg for initial help with DEFORM 2D; Ruben Bjørge for collaborating on TEM analysis; Sindre Bunkholt and Sapthagireesh Subbarayan for help with SEM / EBSD; Qinqlong Zhao for initial help with TEM; Ning Wang for X ray texture measurement; Vinothkumar Palaniswamy for 3 point bend test and light optical microscopy; Chiara Modanese for GDMS; Navaneethan Muthuswamy for DSC and X ray diffraction. Discussions with Sapthagireesh Subbarayan, Sindre Bunkholt and Qinglong Zhao on experimental and characterization techniques have to be appreciated with special thanks.

The encouragement and moral support of Dr R Subramanian, Associate Professor, Department of Metallurgy, PSG College of Technology, Coimbatore, India has helped me a lot during the last three years. His guidance on critical aspects is gratefully acknowledged. I also wish to extend my gratitude to my friends in Trondheim - Balamurgan Loganathan, Dhandapani Kannan and family, Kaushik Jayasayee and

family, Mayilvahanan Alagan Chella, Michal Kolar, Pierre Delaleau, Rajesh Raju, Ralf Beck, Rengarajan Soundararajan, Sapthagireesh Subbarayan and family, Selvanathan Sivalingam and family, Sindre Bunkholt, Valamburi Ganesan and family and Vinothkumar Palanisamy for their pleasant company and for making my stay in Trondheim enjoyable and memorable.

Finally, I wish to thank my family and friends in India for their trust, support and encouragement during the last three years and for their belief that I am still not lost in the North Pole.

ABSTRACT

The work presented in this thesis is an experimental study of roll bonding and accumulative roll bonding of similar and dissimilar metal combinations with special focus on bond strength evaluation, post process heat treatments and layer continuity of the harder phase. Three objectives have been pursued. The first objective was development of a new method to test the bond strength in tensile mode. The second objective was to assess the influence of post deformation heat treatments on the mechanical properties of the material. Hardening on annealing has been mainly investigated in cold rolled and accumulative roll bonded AA3103 aluminium alloy. The third objective was to analyze instabilities and the continuity of the hard layer in accumulative roll bonding of dissimilar material combinations.

The thesis is organized into two parts. The first part is a synopsis that includes the theoretical background and literature review, scope and objectives, a brief description of the various experimental techniques used in the work and concluding remarks. Some recommendations have also been made for future work. The second part of the thesis consists of three articles published or submitted for publication to scientific journals. These articles provide a detailed description of the results of the various experiments carried out with supporting discussion and conclusions.

The first article presents a new method developed for testing the bond strength of roll bonded aluminium sheets in the tensile mode across the interface. Two different aluminium alloys AA3103 & AA1200 in two different temper conditions - 'O' and 'H19' were subjected to roll bonding with progressively increasing thickness reductions and the

tensile bond strength was measured by ripping apart the bonded interface using an adhesive. The influence of the temper conditions and strength of the starting material on the bond strength has been discussed in addition to the effect of increasing deformation.

The second article deals with the hardening on annealing behavior observed in cold rolled and accumulative roll bonded AA3103 alloy. The hardening on annealing behavior is investigated over a broad range of temperatures and annealing times by tensile tests and the effect of strain on the behavior is documented. The contribution of different mechanisms to this behavior is discussed and analyzed. Alloying elements like Si & Mn have been finally reported to contribute significantly to the hardening on annealing in AA3103 alloys by formation of clusters.

The third article presents an investigation on instability and continuity of the hard layer in accumulative roll bonding of dissimilar material combinations. The two dissimilar combinations investigated were AA3103/CuZn20 Brass and AA3103/commercial pure Copper. Tensile tests and three point bend tests are used to investigate the influence of instabilities on the mechanical properties. Numerical simulations of plane strain compression and multi-layer roll bonding using the commercial package DEFORM 2D have been used to observe and analyze the instability mechanism. Applicability of the earlier proposed explanations and mechanisms for necking in the hard layer is discussed and a form of zig-zag instability is suggested to cause the onset of instabilities in the hard layer.

CONTENTS

1. INTRODUCTION

The demands from high performance applications in the aerospace, automotive and industrial domains lay a greater strain on the spectrum of available metals and alloys resulting in an ever increasing demand for light weight yet strong materials. Being a huge consumer of materials, the automotive industry is one potential area where introduction of lightweight materials could result in considerable reduction in CO_2 emissions. Recent reports from the European federation for transport and environment suggest that there has been a 29 % increase in the CO_2 emissions from the transport sector since 1990. The contribution of the transport sector to the EU's CO_2 emissions has increased from 20.5 % in 1990 to 30 % in 2011 [1]. Weight reduction is thus indispensable if carmakers have to reach the target of 130g CO_2 emission per km in the near future. This is due to the fact that for each kg of weight saved, the CO_2 emissions are lowered by 20 kg for a car running an average distance of 170000 km [2].

In addition to reducing the weight in automobiles, an improvement in the efficiency of heat exchangers can greatly contribute to improved efficiency in heat engines. Environmental concern has resulted in development of new heat exchanger materials [3]. Attempts have been made to employ clad materials for heat exchanger applications [4] and many automobile users have started reverting back to copper and brass radiators for automobiles [5] in the aftermarket even though they are heavier. Improvements in the thermal and mechanical properties of aluminium alloys used in heat exchanger applications and development of novel combinations of lightweight materials both for structural and

functional applications by deformation processing may thus contribute significantly to reducing emission of harmful gases.

Aluminium alloys possess good specific strength and corrosion resistance and hence can replace certain steel parts in automobiles and contribute to weight savings. However, the strength requirements of certain structural members in the automotive space frame, pillars and panels are very demanding that use of lightweight aluminium in these areas is almost impossible. Consequently, the need arises for improving the strength of existing lightweight aluminium structures.

Conventional strengthening mechanisms applicable to aluminium alloys like solid solution strengthening, work hardening and precipitation hardening have their own limitations. Although these mechanisms cause considerable strengthening, they cannot improve the properties to match steel. Hence, the need arises for novel processing methods and new techniques to improve properties and performance of available light metals that are not possible to achieve by conventional strengthening mechanisms.

Microstructures with ultra-fine grain sizes in bulk materials have gained popularity because grain refinement is the only method that improves the strength of the material without compromising the ductility and flow properties [6]. Ultra-fine grained metals and alloys show outstanding mechanical properties such as high strength, high toughness and superplasticity at low temperatures [7]. Structural refinement by severe plastic deformation is the most effective method for fabricating these advanced materials in bulk dimensions with a unique combination of properties.

A number of innovative and non-conventional processes for severe plastic deformation like equal channel angular extrusion/pressing (ECAE/ECAP) [8], Multi-axial forging, Cyclic Extrusion and Compression (CEC) [9], High Pressure Torsion (HPT) [10] and Accumulative Roll Bonding (ARB) [7] have evolved. All these processes, except ARB, suffer from two main drawbacks. Firstly, they need forming machines with large load capacities and expensive dies. Secondly, the productivity is very low and the amount of materials produced is very limited. Hence, among different SPD processes for bulk materials, ARB is the only promising process that has a potential for continuous production of large bulk sheet materials for industrial applications [7].

ARB is an intense plastic straining process introducing ultra-high strains in materials. It involves roll bonding of two strips, cutting the rolled material into two equal halves, stacking them one on another and rolling again. This processing sequence of cutting – stacking – rolling illustrated in Fig.1 is repeated a number of times to achieve the desired strain levels. Pre-heating of the samples may be adopted prior to rolling for some materials. The process enables continuous production of bulky materials [7] with ultra-fine grains with large misorientations but with no geometrical shape change in the final strips.

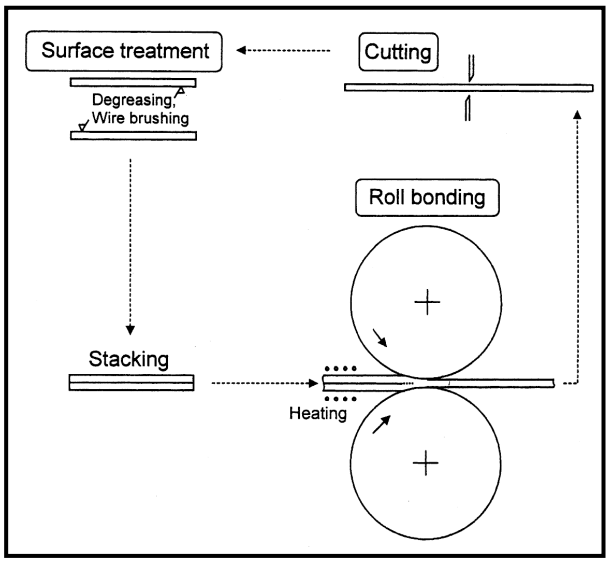

Fig.1.An illustration of the ARB Process [7]

A number of strengthening mechanisms work in tandem in a material processed by ARB. These include grain refinement, strain hardening, severe shear deformation at the sub-surface [7], redundant shear strain due to introduction of severely deformed material in the interior [11], introduction of new interfaces [7] and uniform distribution of oxides & inclusions at the interface. Additionally, low temperature heat treatments have also been reported to cause a slight increase in strength of steel and aluminium severely deformed by ARB [12]. This phenomenon called hardening on annealing has been attributed to the limitation of dislocation sources caused by removal of interior dislocations during the annealing [13]. This low temperature heat treatment thus proves to be another

method to extend further the limits of strength of the severely deformed material.

In addition to producing strong materials, ARB has also been reported to be capable of bonding together dissimilar materials to produce multilayer composites [14-16]. This method of combining dissimilar materials is another prospective way of stretching the mechanical property and applicability limits of light metals. These multilayer metallic materials produced from dissimilar metal combinations combine the unique advantages of the different metals involved to make composites that have better properties than the individual metals and they exhibit unique mechanical, electrical and magnetic properties when the layer thickness reaches the nanometer regime [15].

Thus, ARB process has the potential of exploiting severe plastic deformation both for improving the strength of aluminium and for producing new multilayer materials by combining aluminium with other strong materials to yield composites with better properties. Post ARB heat treatments can also be used to tailor the properties to suitable requirements.

Roll bonding is the first step for any ARB process and qualification of bonds formed in this step are vital for the successful buildup of the ARB process further. A good test for measuring the strength of the bonded materials must allow comparison with the inherent strength of the material [17]. Additionally, a better understanding of the bonding mechanism can only be obtained when the parted surfaces after testing are available intact for microscopic examination. Thus, the need for developing an ideal testing method to assess the bond strength in the

tension mode that could also enable observation of the parted surfaces was recognized as the first step in qualifying and quantifying the roll bonding process.

In this work, attempts are made to develop a testing procedure for bond strength that provides results comparable with the tensile strength of the material. The ability to tailor properties of severely deformed materials by post deformation heat treatments is investigated. Investigations on the hardening on annealing behavior were a consequence of such a study. ARB experiments and numerical simulations are attempted on dissimilar material combinations to produce multi-layer materials and the instability mechanism resulting in disintegration of the hard phase is examined.

2. SCOPE AND OBJECTIVE

The scope of this project is to explore and document the potential of using severe plastic deformation (SPD) for nano-structuring, mechanical alloying and interfacial bonding and the focus has been on developing the ARB process for fabrication of multilayered metal composites to primarily produce new light- weight materials for structural applications. Improvement in properties by post deformation heat treatments is also attempted. According to the scope the following independent objectives have been set.

The first objective was to understand the bonding at the interface of the roll bonded material. To get a good understanding of the bonding at the interface, observation of the parted surfaces of the roll bonded material was essential. Hence, a new method for testing the bond strength in tensile mode became necessary and the tensile bond strength test was developed. The tensile bond strength was measured as a function of increasing strain in AA1200 and AA3103 alloys in the 'O' and 'H19' tempers and the features of the roll bonded interface were examined.

The second objective was to assess the influence of post deformation heat treatments on the mechanical properties of the material deformed both by cold rolling and accumulative roll bonding. Hardening on annealing has been investigated in cold rolled and accumulative roll bonded AA3103 alloy and the various probable mechanisms for this behavior have been discussed with special focus on alloying elements and clustering.

Development of strong yet light-weight structural materials would always require combination of materials with dissimilar strengths and

instabilities are inevitable in co-deformation of dissimilar materials. The third objective was to assess the instability mechanism and its influence on the mechanical properties in ARB of dissimilar material combinations. The experimental work was limited to two dissimilar combinations AA3103 alloy/commercial pure Cu and AA3103 alloy/CuZn20 brass and numerical simulations using the commercial finite element analysis software DEFORM 2D were used for further investigations on the instability mechanism.

3. THEORETICAL BACKGROUND AND LITERATURE REVIEW

3.1. ALUMINIUM ALLOYS

Aluminium in its purest form is soft and has limited practical applications. Hence, it is mixed with small amounts of other elements to make alloys. Addition of these alloying elements makes the resulting alloy very strong. Yet, the alloys retain their light weight property. This high strength –to-weight ratio makes aluminium alloys suitable for use in automobiles and aircrafts where weight is a primary concern. With growing environmental concerns, weight reduction in cars and aircrafts is rigorously attempted and aluminium alloys become the natural material of choice. In addition, Al alloys possess many more advantages over conventional metallic materials like high electrical and thermal conductivities, good formability and excellent recyclability[18]. The ease with which Al alloys can be recycled makes them the preferred material for consumer articles like beverage cans and packaging.

Aluminium alloys are mainly classified in to two groups – cast alloys and wrought alloys [19]. Cast alloys are usually denoted by a designation system #xx.x and wrought alloys are denoted by a system #xxx where #is the number denoting the main group of alloying elements added to the alloy while the remaining numbers denote the amount of alloying elements added. 3XXX will denote a wrought aluminium alloy with Mn as the primary alloying element. A prefix ‘AA’ is used to designate the standard of the Aluminum Association. This type of alloy is non-age hardenable or non-heat treatable which means the alloy cannot be

subjected to any kind of solutionizing and age hardening heat treatments to improve its mechanical properties.

3.2. AA3103 ALUMINIUM ALLOYS

AA3103 aluminium alloys belong to the class of non –heat –treatable aluminium alloys that owe their strength mainly to alloying elements in solid solution, grain size and to particles. Heat treatment of such alloys will usually not produce any precipitates that contribute to strengthening although some dispersoids form in the Al-Mn system [20]. This alloy is used in a wide range of applications where a low to medium strength, good formability and good corrosion resistance are desirable. Some examples are roofing and sidings, corrugated sheets, storage tanks, pipes, heat exchangers, air condition evaporators, motor vehicle radiators, freezer linings, tubing, piping, containers and closures. Mn is added to aluminium usually to control recovery and recrystallization and hence the final grain size and texture in the annealed sheet.

Being an important structural alloy, AA3103 has been extensively used in this work for evaluation of the tensile bond strength, strength improvement by severe plastic deformation and study of the influence of post-deformation heat treatment on mechanical properties and ability to be combined together with other dissimilar materials by deformation processing. Evaluation of the mechanisms that cause property changes during post-deformation heat treatments require an aluminium alloy that is non-heat-treatable. AA3103 alloy was the natural material of choice for such an investigation. The presence of alloying additions in significant quantities provided the additional advantage of a study of influence of these elements on the response to post-deformation heat treatment.

3.3. ROLL BONDING

Roll bonding is the process of bonding together sheets of metal in the solid state by plastic deformation during rolling. If the process is carried out below the recrystallization temperature of the material being deformed, it is called cold roll bonding. In response to the rolling deformation, there occurs expansion of the surfaces in contact which breaks up the surface layer or the thin film of oxides and contaminants. Moreover, the normal pressure from the rolls causes extrusion of the virgin material through these surface cracks and brings it within atomic distances thus resulting in bonding [17, 21, 22]. Thus coalescence caused by joint plastic deformation of the two surfaces in contact is essential for cold welding to occur at the interface.

The degree of deformation expressed by surface exposure 'Y' of the weld interface is the basic variable governing coalescence.

$$Y = \frac{A_1 - A_0}{A_1}$$

where A_0 is the initial and A_1 is the final area of the weld interface . In the case of rolling, the rolling reduction 'R' is considered to be the surface exposure 'Y' and bonding is usually reported to occur only after a threshold deformation is reached. Scratch brushing produces a work hardened surface layer and exposure of the base material by fracture of this layer is what governs coalescence and bond formation at the interface [22]. Scratch brushing has been reported to be an effective form of surface preparation for cold welding because it removes the surface contaminants and forms hard layers on the surfaces to be welded which

adhere and further behave as a single layer thereby exposing maximum area of virgin metal for potential bonding [23]. Fig.2 shows the effect of different surface preparations on the shear strength of the bonds in roll bonded aluminium.

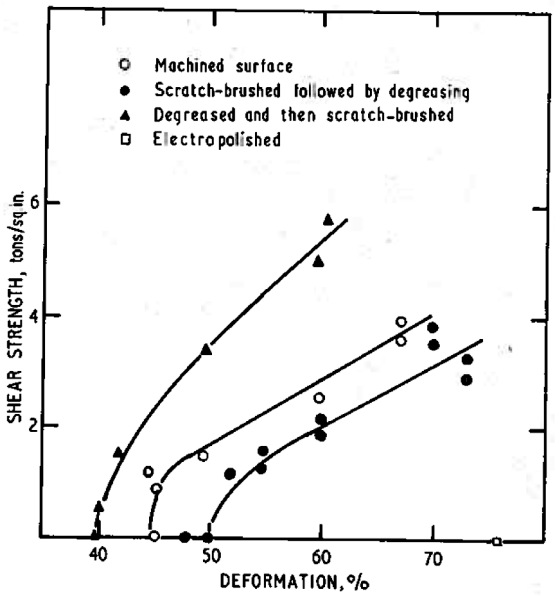

Fig.2. Effect of different types of surface preparation on the shear strength of bonds in roll bonded aluminium composites [23]

According to Bay et.al [21, 22] , the basic mechanism of metallic bond formation in cold welding involves the following steps

1) Fracture of the brittle cover layer / the contaminant surface film
2) Extrusion of base material through the cracks
3) Build-up of contact with the base material of the opposite surface
4) Coalescence with the base material of the opposite surface

A schematic outline of these steps is provided in Fig.3.

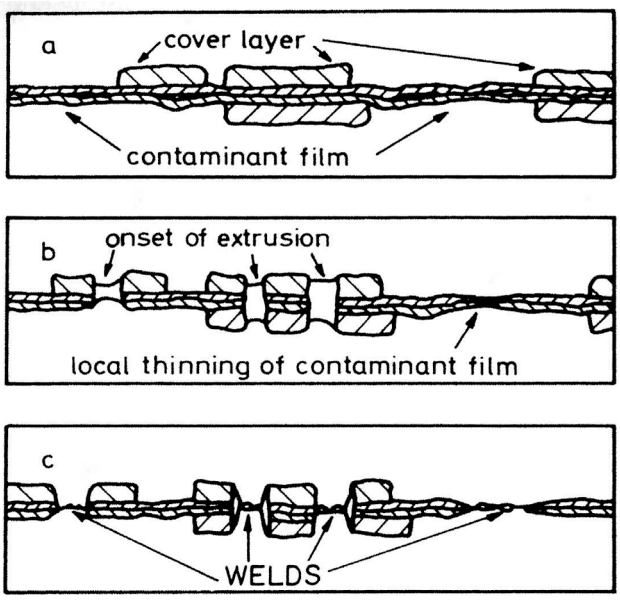

Fig.3. Schematic outline of the different steps involved in bond formation at the interface:- a) break-up of cover layer b) extrusion onset c) weld formation [22]

The fracture of the surface layer can in turn occur in two different modes depending on the type of the surface layer present [22].

1) Fracture of the brittle cover layer and extrusion of the base metal through the cracks and establishment of contact and coalescence
2) Fracture of the contaminant film and establishment of contact and coalescence

After de-covering by one of the above fracture mechanisms, the virgin material at the interface is protected from atmospheric contamination by high pressure at the interface. Followed by this, further surface expansion and extrusion causes contact to be established at the highest asperities of the de-covered virgin material and coalescence occurs when the layers come within atomic distances.

Based on these two mechanisms, a theoretical model for the strength of the weld has been proposed [22]

$$\frac{\sigma_b}{\sigma_o} = (1-\beta)Y\frac{p-p_E}{\sigma_o} + \beta\frac{Y-Y'}{1-Y'}\frac{p}{\sigma_o}$$

where,

σ_b is the strength of the weld

σ_o is the yield strength of the base material

β is the square of the fraction of the film layer to total area

Y is the surface exposure

Y' is the threshold surface exposure of the contaminant film

P is the normal pressure at the base metal surface

P_E is the extrusion pressure

It has been reported that fracture of the brittle cover layer formed by scratch brushing is usually active over 60 % of the total area at the interface and for Al-Al cold welding, the threshold surface exposure of the contaminant film for bonding to occur Y' is 0.35 [22].

A number of parameters like the deformation/surface expansion, the strength and the hardness of the starting material, temperature and time of roll bonding, normal pressure, crystal structure of the bonding materials, physical properties of the contaminant surface film and surface preparation prior to roll bonding are reported to affect the strength of the bond [17, 21, 22, 24]. According to Vaidyanath et.al, with increasing deformation, the bond strength of a roll bonded composite increases and tends to reach the strength of the solid material deformed to a similar level [17]. Fig.4 presents differences in bond strengths as measured by peel test between starting materials of different strengths. Fig.5 shows that the threshold deformation for formation of bonds in aluminium decreases with increasing processing temperature. While the influence of these parameters on the bond strength has not been completely investigated, finding a method to precisely assess the strength of the bond has also remained a challenge.

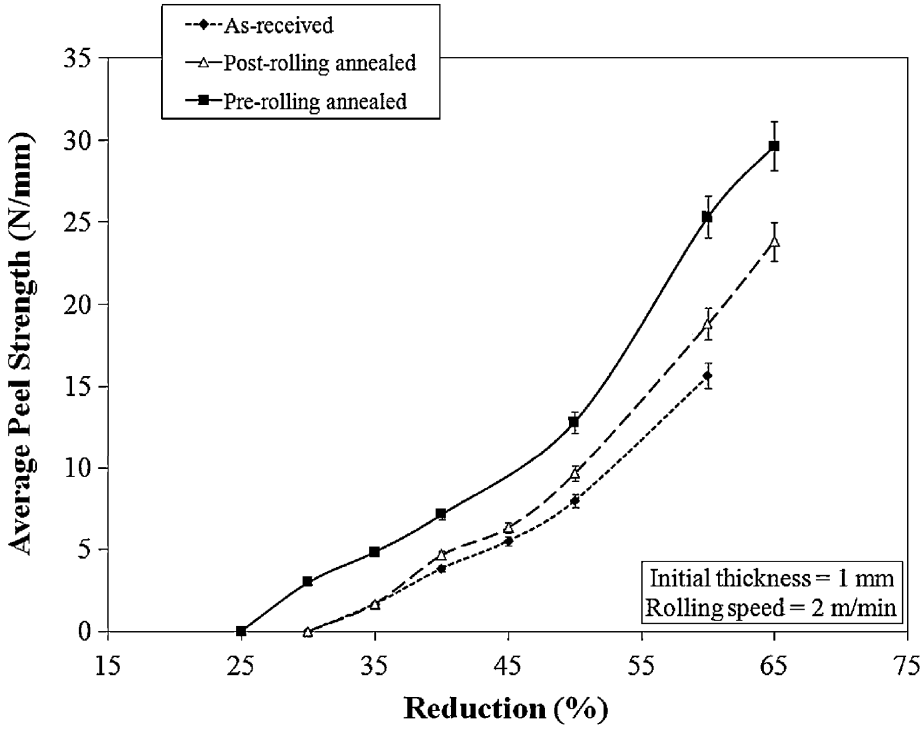

Fig.4. Effect of pre and post roll bonding annealing on the peel strength of roll bonded aluminium [24]

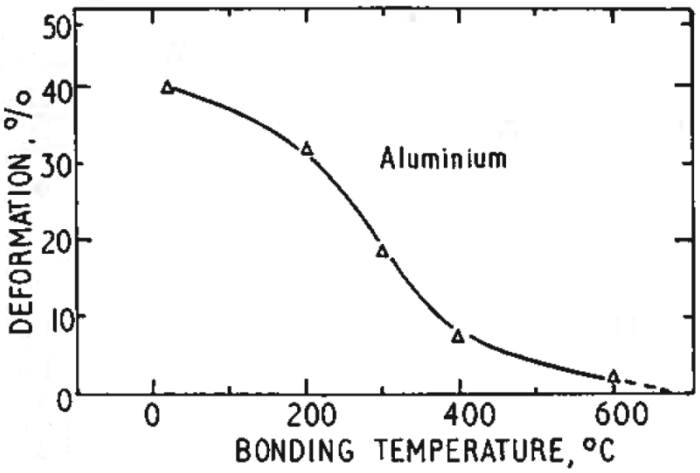

Fig.5. Variation of threshold deformation for bond formation in aluminium with temperature [17]

3.4. MEASUREMENT OF BOND STRENGTH IN ROLL BONDED MATERIAL

Measurement of bond strength of roll bonded materials has been reportedly done by three methods

1) Reverse Bend Test
2) Peel Test
3) Shear test

In the reverse bend test illustrated in Fig.6, a specimen of dimensions 20mm X 80mm is alternately bent to ± 90° until delamination occurs in the interface or fracture occurs in the strip. A qualitative measure of the bond strength can be obtained from the number of bendings for failure [25].

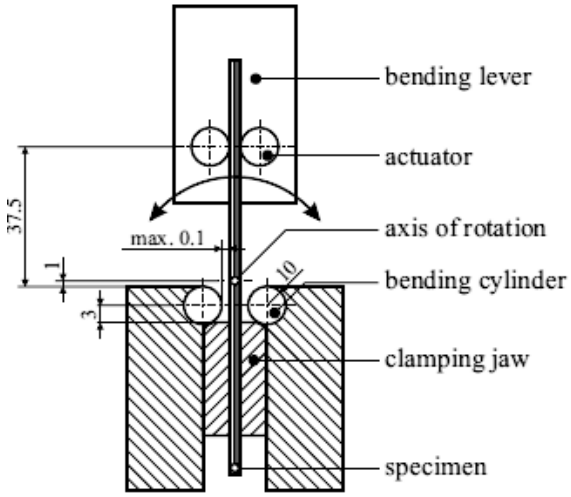

Fig.6. Schematic - reverse bend test set up [25]

The peel test gives a more quantitative measure of the bond strength. This test involves peeling open the two parted ends of a roll bonded strip in the tensile mode as shown in Fig.7. This method is based on the ASTM

1876 -72 standard for testing peel strength of adhesives. The average peel force measured over a certain length of peeling the sample is used to calculate the average peel strength. Although this test gives a measured strength, it suffers from a number of drawbacks. First, the peeling forces vary along the length of the bonded specimen and the results are consequently based on average values. The test can be applied to compare a range of bond strengths for different surface preparations or to measure the critical rolling reduction required for bonding but the outcome of the test cannot be directly related to one specific bonding property. Also, the final thickness of the strips should be identical to avoid comparing different contributions from the plastic and elastic parts of the involved deformations. Further, an upper limit exists for the tensile force that can be applied in this test before a failure occurs in one of the strips because the thickness of the two peeled strips is about half of the original strip thickness.

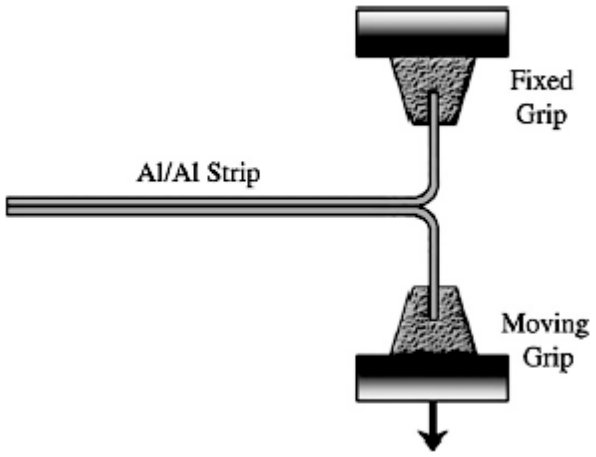

Fig.7. Schematic – Peel test for bond strength [24]

The third, most popular method for assessing the bond strength is the shear test. A schematic of the shear test sample is given in Fig.8. In this test, a tensile specimen with offset slots normal to the bonded interface on opposite sides of the roll bonded material with certain spacing between them is used. The bonded surfaces between the slots are subjected to a shear load during the pulling of the specimen in tensile mode. The outcome of this test is an estimate of the shear strength of the bond. Although this test appears more quantitative than the other two, it still suffers from a number of drawbacks. Sample preparation for this test is very challenging as precise slots are to be machined on thin samples. The results are very sensitive to the length of the bonded interface under test and sample dimensions are to be considerably altered to test samples of different strength levels. There occurs considerable bending and un-bending during the test and consequently the calculated shear stress is not the pure shear stress but a shear stress component where other stress components are considerably smaller.

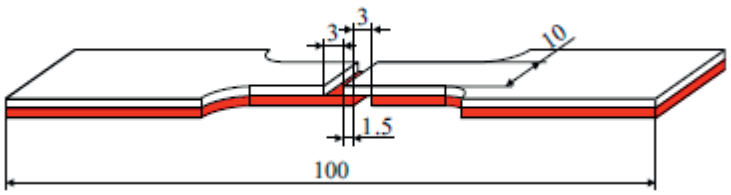

Fig.8. Specimen for testing of bond shear strength [25]

All these three methods discussed above suffer from one common drawback. They do not provide results that can be directly compared with

the inherent strength of the material in tension mode. Due to the complex stress states involved in these tests, the parted surfaces after testing cannot be really used to understand the bonding mechanism. Hence, the need for an ideal testing method to assess the bond strength in tension mode where the parted surfaces are available for microscopic examination was recognised and the tensile bond strength test described in article I was developed.

3.5. ACCUMULATIVE ROLL BONDING

Accumulative roll bonding is an extension of the conventional roll bonding process to achieve nano-structuring and improved mechanical properties in materials. Developed by Saito and Tsuji [7] in 1998, this technique involves preparing the surfaces and roll bonding of two strips followed by a repetition of cutting the roll bonded sheet into two halves, preparing their surfaces and roll bonding them again. The process sequence of cutting – surface preparation – stacking – roll bonding constitutes one cycle of ARB and the sequence is repeated a number of times to achieve desired levels of nano-structuring and strengthening. The process has attracted considerable interest in recent years because of its inherent advantages over other severe plastic deformation techniques like low friction, large specimen dimensions and the ability to produce bulk materials on an industrial scale. Because the sheets are cut into two and stacked again, the original sheet thickness is preserved and the absence of a geometrical shape change serves to be another advantage of the process.

The process of ARB has been successfully used to produce high strength commercial pure aluminium, Al-Mg alloy and IF steel sheets. Moreover,

ARB has also helped improve the strength of oxygen free high conductivity Cu, Ni, SS400 steel considerably [26]. Since materials processed by ARB are mostly ultra-fine grain materials, they possess outstanding strengths at ambient temperatures combined with good super-plastic deformation capabilities at elevated temperatures. By virtue of this exotic combination of properties, these materials deem to be called 'supermetals'.

Generally, in the ARB process, the extent to which the material can be strained is unlimited because the number of times the ARB cycle can be repeated is limitless. Nevertheless, consideration of practical factors like strain hardening, normal pressure requirements and edge cracking limits the maximum number of ARB cycles applicable. A reduction of 50% is usually applied in each cycle of ARB. With this kind of reduction, the thickness of the strip 't' after 'n' cycles is

$$t = \frac{t_0}{2^n}$$

where t_0 is the initial thickness of the strips.

After 'n' cycles, the total reduction r_t is given by

$$r_t = 1 - \frac{t}{t_0} = 1 - \frac{1}{2^n}$$

The equivalent plastic strain ε assuming von Mises yield criterion and plane strain condition is given by

$$\varepsilon = \left(\frac{2}{\sqrt{3}} \ln\left(\frac{1}{2} \right) \right) n = 0.8n \quad [7]$$

Thus, this process is capable of reducing a 1 mm thick sheet to approximately 1 μm after 10 cycles of ARB. An example of the changes in the geometry when two 1 mm thick sheets are rolled bonded with a 50 % deformation in each ARB cycle is provided in Table 1.

No. of cycles	1	2	3	4	5	6	7	8	9	10	n
No. of layers	2	4	8	16	32	64	128	256	512	1024	2^n
No of bonded boundaries	1	3	7	15	31	63	127	255	511	1023	2^n-1
Layer interval (μm)	500	250	125	62.5	31.2	15.6	7.8	3.9	1.9	0.96	$1000/2^n$
Total reduction (%)	50	75	87.5	93.8	96.9	98.4	99.2	99.6	99.8	99.9	$(1-1/2^n)\times 100$
Equivalent strain	0.8	1.6	2.4	3.2	4.0	4.8	5.6	6.4	7.2	8.0	$\left(\frac{2}{\sqrt{3}}\ln 2\right) n = 0.8\,n$

Table 1. Changes in geometry of materials during ARB of two 1 mm sheets with a 50 % reduction per cycle [26]

Improvements in mechanical properties of ARB AA1100 aluminium are illustrated in Fig.9. It can be observed that the tensile strength increases considerably with increasing number of ARB cycles. These surprising levels of strength are not possible to reach by conventional grain refinement and strain hardening mechanisms which gives an indication that that a synergy between many other different mechanisms must act. The ARB process thus differs from other severe plastic deformation processes in terms of the strengthening mechanisms. In addition to conventional grain refinement and strain hardening, there are a host of other mechanisms like improved grain refinement due to severe shear deformation below the surface caused by increased friction between the work piece and the roll, introduction of severely deformed material in the interior due to repetitive cutting and stacking prior to rolling, introduction of new interfaces and a uniform dispersion of oxide films on the surface

and inclusions that prevent grain growth [7]. The absence of these mechanisms is what makes conventional rolling quite inferior to ARB.

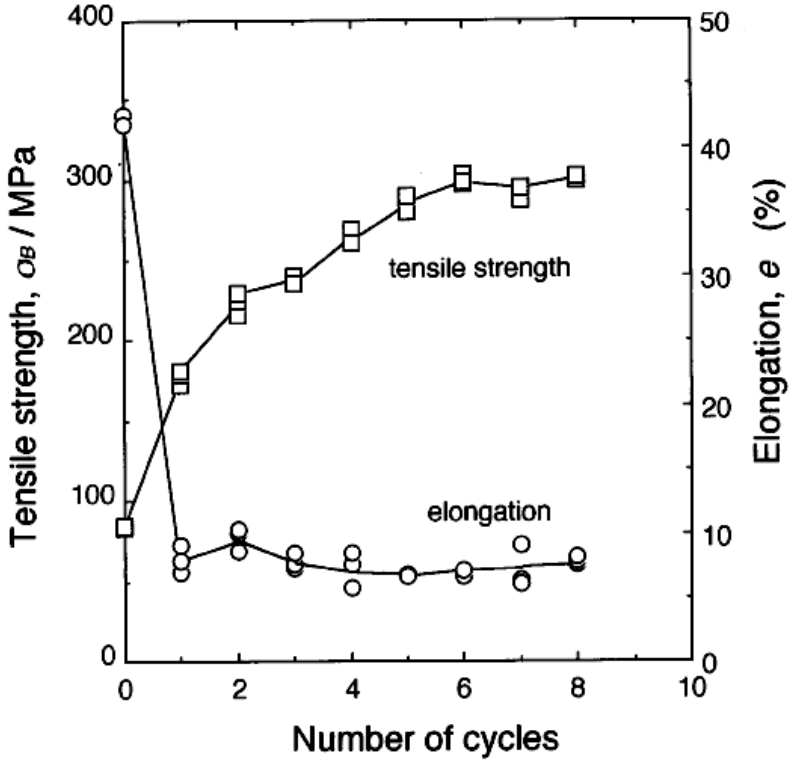

Fig.9. Changes in mechanical properties of AA1100 aluminium alloy with increasing number of cycles of ARB at 200°C [27]

The evolution of the microstructure during ARB of commercial purity aluminium has been documented by Huang et.al [28]. The microstructure is usually characterized by two types of boundaries- the long lamellar boundaries running parallel to the rolling plane and the short transverse boundaries interconnecting the lamellar boundaries. With an increase in strain in ARB, the spacing between the lamellar and interconnecting

boundaries and their aspect ratio are reported to decrease and the misorientation angle across these boundaries increases. No saturation has been observed in the decrease of lamellar and interconnecting boundaries but the increase in the misorientation angle saturates. Fig.10 presents a TEM image of lamellar structure in ARBed commercial pure Al and also an illustration of the different types of boundaries.

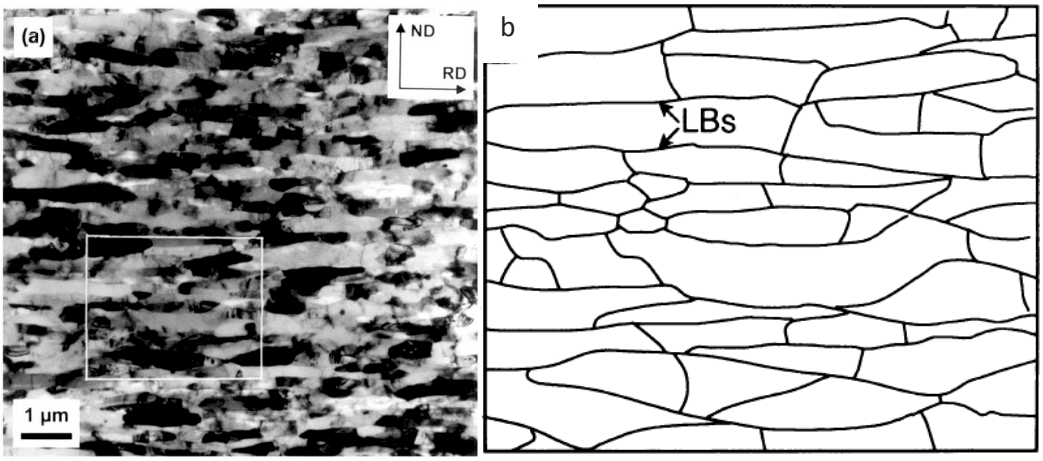

Fig.10.a) TEM micrograph of lamellar structure in ARB ‘ed commercial purity aluminium b) Schematic of lamellar boundaries (LB’s) and transverse interconnecting boundaries [28]

Although structural evolution during ARB is considered to resemble structural evolution during cold rolling, certain notable differences have been observed. At any given level of equivalent strain, the boundary spacing in ARB specimen is always observed to be smaller than that in a cold rolled specimen and larger misorientation angles and angular saturation is usually observed in ARB aluminium but not in cold rolled aluminium [28]. Another factor that needs to be considered is the effect of redundant shear strain in ARB. Both the geometrical and frictional

manifestations of the shear strain augment the grain refinement and contribute to improved properties but shear strain also causes a great amount of heterogeneity in the microstructure and texture across the thickness of the specimen [29]. This heterogeneity is another factor that distinguishes cold rolled microsctructures from ARB microstructures.

By virtue of the unique features discussed above, ARB has proven itself to be one of the most versatile SPD techniques developed in recent times. ARB has been successfully used for a wide variety of applications ranging from microstructural and property refinement to synthesis of closed cell aluminium foam [30]. Koizumi et.al have reported an improvement in the damping capacity of ultra-fine grained aluminium produced by ARB process [31]. The availability of new interfaces in every cycle has facilitated the use of blowing agent like TiH_2 in between aluminium layers for manufacture of closed-cell foams [30] . Surprising levels of mechanical properties have been reached by subjecting a variety of metals like Al and Al alloys, Ni, Ti, oxygen free high conductivity Cu and interstitial free (IF) steel to ARB [26]. These indicate that the potential of ARB in producing materials with unique combination of properties is intense. Further heat treatments on materials severely deformed by ARB could either help tailor the properties of these materials to specific requirements or can also open up new dimensions of properties that are otherwise not achievable by conventional processing. Thus the spectrum of applicability of these materials can get extended further.

Processing materials by ARB has its own limitations also. Materials severely deformed by ARB possess limited ductility and formability and

optimization of properties by post –processing heat treatments are necessary. Difficulties with steps in ARB processing such as obtaining the optimum surface roughness after wire brushing, contamination of the degreased and wire brushed surfaces, the short time duration for roll bonding after surface preparation and the tendency of the strips to develop transverse cracks make obtaining sound samples even more challenging. Residual oxides and contaminants can also get entrapped at the roll bonded interface and brittle intermetallics can form between reactive metal combinations in hot ARB, thus affecting the bonding and integrity of the samples. Additionally, redundant shear strain gets distributed in a complicated fashion through the thickness of the ARB strips causing severe inhomogeneity in the microstructure and texture [11, 32].

3.6. HEAT TREATMENT OF ARB MATERIAL - HARDENING ON ANNEALING (HOA)

The severe strains introduced during processing render materials subjected to ARB to exhibit a great increase in strength and decrease in ductility when compared to the starting material. To optimize the strength and ductility, the logical step ahead would be to subject the material to an annealing treatment. However, in sharp contrast to the conventional property changes associated with annealing, it has been reported that commercial purity Al subjected to ARB exhibits an increase in strength and a loss of ductility after a low temperature annealing treatment. This and its associated phenomenon of decrease in strength on subsequent cold rolling after the annealing were reported to be the hardening on annealing and softening on deformation behaviour exhibited by nanostructured materials [12, 13].

The temperatures used for such annealing treatments are low enough not to cause recrystallization but sufficient to cause coarsening of boundary spacing, recovery of low angle grain boundaries and reduction in dislocation density in the grain interior, grain boundaries and triple junctions. Materials deformed by conventional deformation processes have grain sizes that are usually not in the in the nano-meter range and the microstructural changes mentioned above would cause softening. However, in a nanostructured material, these changes may produce a different effect. The small gran size results in availability of closely spaced high angle grain boundaries (HAGB's) which act as active sinks for the dislocation annihilation during the annealing treatment [13]. In ARB material, the high angle lamellar boundaries are spaced so close that annihilation of interior dislocations occurs readily. Consequently, activation of new dislocation sources during further straining occurs at higher stresses and the yield stress of the material is increased.

Figure 11 illustrates the hardening on annealing behaviour in commercial pure nanostructured aluminium. This behaviour is attributed to the limitation of dislocation sources i.e. the reduction in generation and interaction of dislocations by the annealing treatment. A subsequent deformation step as shown in Fig.12 was reported to have restored the dislocation structure and facilitated the yielding process resulting in a strength decrease and ductility increase. Annealing causes a decrease in the interior dislocation density resulting in dislocation source limited hardening and the subsequent cold rolling re-introduces the dislocations in the structure causing softening on deformation [33]. By carefully playing around with the levels of deformation in ARB, heat treatment parameters after ARB and the small deformation post annealing, it

becomes possible to alter the strength and tailor the properties of the material to suit a wide range of requirements and applications. Thus the range of applicability of the ARB material can be expanded greatly.

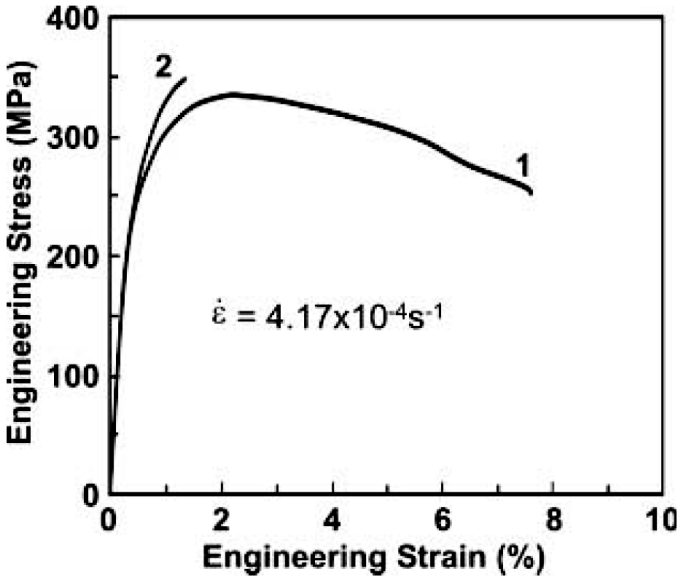

Fig.11. Stress-strain curves of commercial pure aluminium processed by ARB, curve 1: as deformed to 6 cycles, curve 2: deformed to 6 cycles followed by annealing at 150°C, for 30 mins [13]

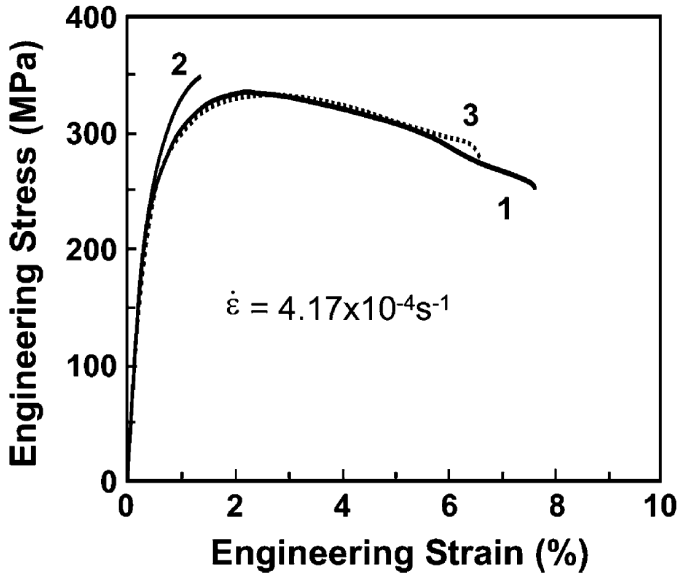

Fig.12. Stress-strain curves of commercial pure aluminium processed by ARB, curve 1: as deformed to 6 cycles, curve 2: deformed to 6 cycles followed by annealing at 150°C, for 30 mins, curve 3: deformed to 15 % by cold rolling after processing similar to curve 2 [33]

3.7. ARB OF DISSIMILAR MATERIAL COMBINATIONS

While ARB of similar metal combinations like aluminium and steel has resulted in drastic improvement in properties of these materials [7, 27], combining together two dissimilar materials that are otherwise difficult to bond together has also been explored [14, 15, 34]. Such combinations of dissimilar materials by ARB open out vast avenues for new applications of material like functionally graded materials, deformation induced synthesis and transformation of multilayer materials, solid state amorphization and mechanical alloying of different materials in addition to synthesis of nanostructured materials and structural composites.

Traditionally, most of these multilayer materials have been produced by bottom-up processes like vapor deposition or epitaxial growth which are expensive and time-consuming [35, 36]. Unfortunately, these methods do not have the capabilities to produce products on a very large scale or in significant quantities. With the development of deformation synthesis techniques for multilayers like repeated folding and rolling or ARB, it has been possible to produce these multilayer materials on a bulk scale in sizes suitable for structural or industrial use [14-16].

Metal intermetallic laminates have been successfully produced by ARB of IF steel and aluminium [37, 38]. By combining together dissimilar materials like Al/Cu [15], Mg/Al [14], Ti/Al [34] ARB has attempted to exploit the best properties of the individual materials in the combination and thereby produce multilayer composites with unique properties. Additionally, bulk mechanical alloying of Cu-Ag with Cu/Zr [39] and solid state amorphization in Zr based binary systems [40] have also been attempted by ARB of dissimilar material combinations.

Another very unique feature of cold roll bonded laminated composites is their enhanced toughness and fatigue strength. Outstanding Charpy impact values have been reported on multilayer aluminium composites in the “crack arrester orientation”. This has been attributed to the mechanism of interface pre-delamination and crack re-nucleation in every layer of the composite laminate [41, 42]. Additionally, a mechanical contrast between the constituent layers has been reported to improve the toughness in addition to improving the fatigue strength significantly in cold roll bonded Cu/Cu laminated composites [43].

Retardation of cracking induced by local interface delamination and the secondary initiation of fatigue cracks at the inner layer surfaces have been reported to be the main mechanisms. Thus, a multilayer composite with a mechanical contrast becomes an ideal material for use in severe impact and fatigue load conditions.

By its inherent ability to bond together dissimilar materials, ARB can introduce a mechanical contrast easily in the composite being fabricated. However, when two metals with difference in flow properties undergo co-deformation, plastic instabilities are prone to occur and the hard phase usually necks and ruptures leaving behind a dispersion of the hard phase in the matrix [44-46]. This type of composite may be suitable for certain applications where layer continuity is not important like mechanical alloying, but other applications that require precise load re-distribution between the constituent layers demand layer continuity. Further, necking in the hard layer can pose as a big challenge for refining thickness down to nano-scale and the improved fatigue strength and toughness of a multi-layer roll bonded material can be exploited only when the layers are continuous. Fig.13 shows necking in Al/Ni composite as early as after 1 cycle of ARB. Control of layer continuity in metallic multilayers is thus an important aspect to realize functional advantages.

Deformation of sandwich materials has been widely investigated and a number of deformation models have been developed to predict the flow behavior of the different materials in plane strain compression and rolling. These models usually assume isostrain conditions and show that in-plane stresses which are compressive in the softer component and tensile in the harder component are developed to satisfy yield conditions

[47]. Such tensile stresses in the harder component are usually considered to cause unstable flow and failure [48]. Since ARB of dissimilar materials is an extended case of sandwich sheet rolling, these models and their predictions may be applied, although with caution, to understand the deformation behavior of the hard layer.

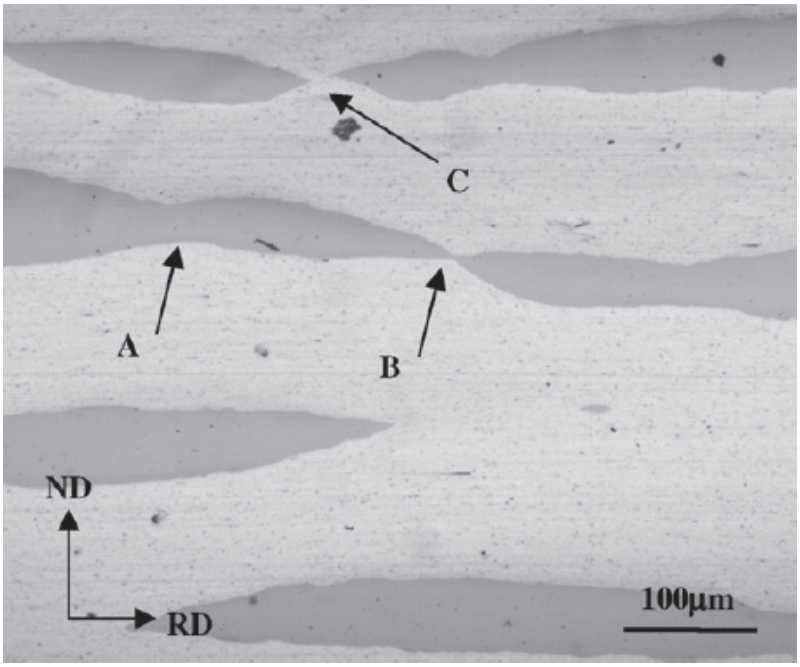

Fig.13. Optical microstructure of Al/Ni composite after 1 cycle ARB, showing necking (A), fracturing (B), and departing(C) of Ni layers [16]

In a multilayer composite made up of dissimilar materials, when a neck forms in the hard layer, localized deformation and preferential strain hardening of the soft matrix occurs in the vicinity of this neck. The strain hardened matrix can support more load to resist further deformation and subsequent necking will occur locally along the entire length of the layer.

This causes multiple necking in the hard phase. Deformability of the hard phase is thus reported to be the determining factor that controls multiple necking and layer continuity in this case [49]. Plastic instability criteria for diffuse necking and local necking have also been developed to predict the occurrence of plastic instability during rolling of sandwich sheets bonded initially. The occurrence of plastic instability for local necking is concluded to be dependent on the strain hardening exponent of the hard layer, whereas, that for diffuse necking is dependent on initial thickness ratio, strength coefficients and strain hardening exponents of both the hard and soft layers [50].

Dissimilar material combinations that undergo severe deformation in processes like ARB usually exhibit two different types of morphological features:- one where the continuity of the layers is maintained until layer thickness reduces to nano-scale and the other where the hard layers neck and rupture [46]. Fe/Cu, Fe/Ag and Cu/Brass are examples of the former case. The necking of the hard layer can further occur in two different ways. In systems like Al/Cu, the hard Cu layer has been reported to undergo multiple necking and extensive elongation down to sub-micrometer thickness whereas in systems like Pd/Sn there occurs very small thickness reduction of the hard layer and the hard layer undergoes multiple fracture-rupture resulting in a saucer-like microstructure [44, 46].

Factors like the crystalline structure of the constituent materials, the processing temperature, the interface bonding effects, the flow properties of the hard and soft phase and the initial thickness ratio of the constituent phases are considered to affect the layer continuity [44, 46]. Of these, the

strength coefficient and strain hardening exponent of the hard phase and the initial thickness ratio of the constituent phases are considered to greatly influence the critical reduction for necking in the hard phase [46]. Many criteria have been proposed to predict the layer continuity in multilayers based on analytical models. Plastic instability in the hard phase is usually considered to become greater due to the stress concentration around the neck as necking progresses and work hardening of the soft phase in the vicinity of the neck causes preferential strain hardening thereby supporting the load to resist more deformation around the neck [49]. Consequently, flow properties of the constituent phases are an important factor to be considered in the viewpoint of layer continuity. A homogenous refinement of the microstructure in deformation processing has been predicted based on numerical simulations for continuously reinforced systems when the flow stress ratio of the constituent phases is between 2 and 5 [51]. Another criterion based on the thickness ratio of the hard layer to the thickness of the total stack predicts a larger thickness reduction for occurrence of necking with a larger thickness ratio [46]. Bordeaux and Yavari [49] in their model for multiple necking have considered only the flow properties of the hard phase and stated that multiple necking conditions are easily attained when the hard phase is softer.

Although much has been reported on the necking and rupture in the hard layer and some attempts have been made to predict the criteria for layer continuity, the effect of processing temperature, pre roll bonding heat treatment and mixed mode processing route has not been investigated especially on the strain redistribution between the layers. Further, quantifying strain re-distribution between the hard and the soft layer and

observing the effect of interface bonding characteristics on the disintegration of the hard phase remains to be a big challenge.

3.8. DEFORMATION SIMULATIONS

Structural evolution at the continuum level influences to a great extent the fine scale structures that form after severe deformation and hence affect the functionality of the multilayer material. Control of macrostructure of multi-layers is thus important. The simplest way to study the deformation behavior of multi-layer materials in the macro scale is to use simulations. Deformation simulations using finite element methods (FEM) have been used to examine multi-layer materials with both continuous and discontinuous reinforcements [51]. In these simulations, the reinforcement to matrix flow stress ratio is varied and optimum values for homogeneous reinforcement in laminates with both continuous and discontinuous reinforcement are predicted.

Two dimensional plane-strain models are shown to provide much of the necessary information required to study deformation in multi-layer laminates [51]. Geometrical parameters like the thickness and relative spacing of the hard reinforcement in the case of a continuous reinforcement and an additional aspect ratio in the case of a discontinuous reinforcement can be used to capture strain and strain redistribution between the layers and homogeneity of deformation. Usually, when the reinforcement deforms more than the matrix, it develops necks periodically along its length. These necks may or may not

be stable depending on the extent to which the reinforcement undergoes deformation relative to the whole composite.

In simulations of deformation in a continuously reinforced system, sinusoidal thickness variations with a small amplitude and wavelength comparable to the layer thickness are introduced to generate disturbances in the analysis and destabilize the homogeneity of the deformation. Periodic stable necks were reported to form in the hard layer without disrupting the continuity of the structure as long as the strain hardening in both the layers remained as low as 0.2 and the strain in the reinforcement was not much higher than the strain in the matrix [51]. Conditions for homogeneous deformation and macrostructure control based on the flow stress ratio have also been predicted by such simulations. Accordingly, a homogeneous refinement of macrostructure was possible in deformation processing for both continuous and discontinuous reinforcements in a soft matrix as long as the flow stress ratio of the reinforcement to the matrix was at most 2 for the ideal plastic case and 5 for the case with work hardening [51].

4. EXPERIMENTS

The procedure adopted for preparing different materials, description of equipment and the various characterization techniques used for analysis of mechanical properties and microstructural features are presented in this section.

4.1. ROLL BONDING AND ACCUMULATIVE ROLL BONDING

The general procedure adopted for roll bonding and accumulative roll bonding is described in this section. The first step in the roll bonding or accumulative roll bonding process is surface preparation. Degreasing and wire brushing was chosen to be the optimum surface preparation technique after Vaidyanath et.al [23]. Fig.14 shows the equipment used and the procedure for surface preparation.

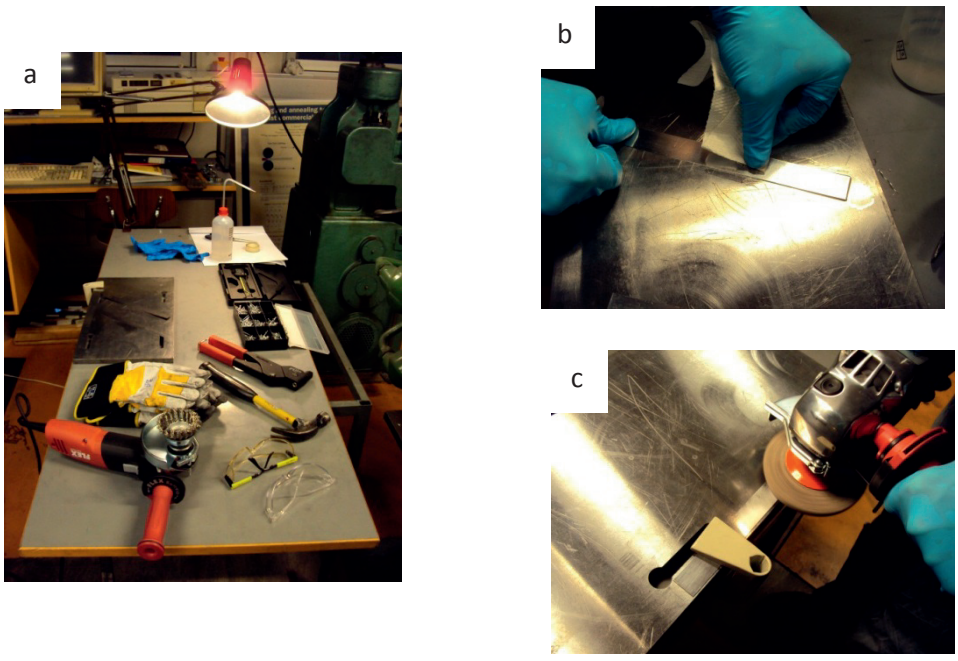

Fig.14. a) Surface preparation equipment, b) degreasing and c) wire brushing process

The strips for roll bonding were first degreased with acetone until no visible dirt or grease was observed on the surface. Degreasing was attempted with ethanol but that resulted in poor bonding at the interface. Consequently, acetone was chosen as the degreasing medium because of its inherent ability to dissolve most oils and greases and its ability to dry up fast from the surface. Followed by degreasing, the strips were clamped to a flat surface and subjected to wire brushing. A rotary wire brush attached to a FLEX LE 14-7 125 INOX angle grinder revolving at a speed of 3800 rpm was used for the purpose. The speed of 3800 rpm was chosen based on considerations that the speed ought to be sufficient to provide a work hardened layer on the strip surface and cause removal of adsorbed moisture but not too high to cause excessive plastic deformation and gouging.

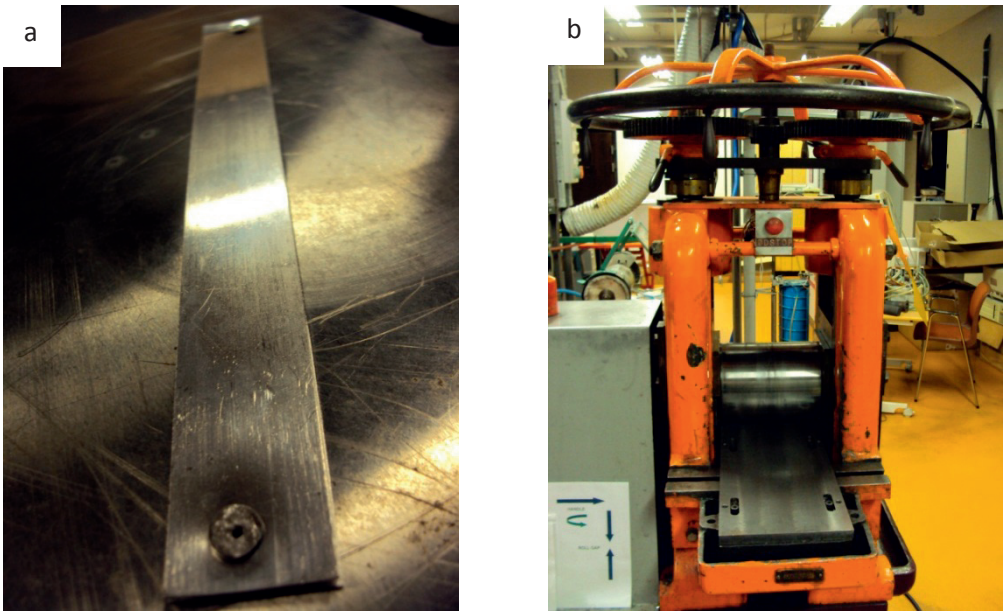

Fig.15. a) Riveted stack ready for roll bonding b) 2 high rolling mill used for roll bonding

After preparing the surfaces, the strips were riveted at the two ends to prevent parting during roll bonding as shown in Fig.15.a. For cold roll bonding, the strip stack was fed into the rolls within 2 minutes after the surface preparation to avoid contamination and moisture adsorption at the interface. In the case of warm roll bonding, the stack was preheated in an oven at the required temperature and then fed into the rolls. The peripheral speed of the rolls was maintained at 27 mm/s for cold roll bonding and 67 mm/s for warm roll bonding. Roll bonding was carried out in a 2 high rolling mill with a roll diameter of 205 mm shown in Fig.15.b. The roll separation was controlled by the handles to provide the reduction required for the different roll bonding steps.

For accumulative roll bonding, the strips after the first roll bonding step were cut into two halves and the bonding surfaces were subjected to the same degreasing and wire brushing steps as described above. These were followed by riveting and roll bonding of the stack. Preheating of the stack was used as and when required and a constant reduction of 50 % was always maintained in each cycle of roll bonding.

4.2. MECHANICAL TESTS

4.2.1. TENSILE TEST

Uniaxial tensile testing provides a precise estimate of mechanical properties of the material. Therefore, tensile tests have been mainly used to assess the property changes in response to increasing levels of deformation and different heat treatments in this work. All the tensile tests have been carried out according to ASTM E 8-M standards. Tensile test specimens have been machined according to the standard in certain

cases and in the other cases some scaled-down versions have been used. All the tensile tests have been carried out on a servo-hydraulic MTS 810 universal testing machine. Test data was collected using the MTS TestStar and TestWorks 4 software. All the tests have been carried out at a constant crosshead speed of 2 mm/min and extensometers with 15 mm and 25 mm gauge length have been used to capture the elongation depending on the requirement.

4.2.2. THREE POINT BEND TEST

The deformation mode that a sheet metal component experiences in actual applications is different from that in the case of uniaxial tension. Hence, tensile strength cannot be directly used for material selection and design. Additionally, deformation of multilayer materials in tension is influenced by a number of factors like residual stresses, plastic anisotropy differences and interface delamination [52]. Three point bending could provide some insight into the bendability and formability of sheet materials into components in addition to giving information on flexural strength and ductility. The applicability of multilayer sheet materials in certain structural applications can be assessed by such tests. The three point bend tests in this work have been carried out on ARB'ed dissimilar sheet specimens in the crack arrester morphology with the bending load acting along the normal direction in the rolling direction (RD) – normal direction plane (ND) (Fig.16). The samples were subjected to bending at a constant stroke rate of 2.4 mm/ min up to a displacement of 8 mm and the force and displacement were recorded. Both the force and displacement were normalized with respect to the sample thickness and nominal flexural strength- nominal displacement curves were plotted.

The objective of using nominal values is to make comparison of samples of different thicknesses possible. Steps in the loading curve were precisely captured to obtain loads at which delamination occurred.

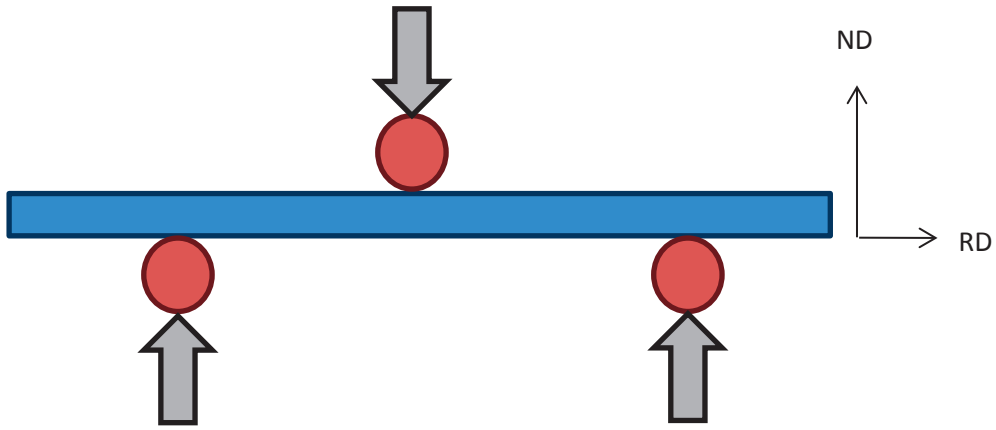

Fig.16. Schematic of 3 point bend test in the RD-ND plane

4.2.3. TENSILE BOND STRENGTH TEST

The new test method developed to measure the bond strength of roll bonded samples in the tension mode involved a special sample preparation procedure. Coin samples of 15 mm diameter were machined out from the roll bonded strips. The opposite faces of the coin samples were cleaned, degreased using acetone and then roughened over a 320 grit emery strip. The prepared faces of the sample were glued to two aluminium rods of 15 mm diameter using Loctite Hysol 9466 A & B epoxy glue. The combination of rods glued to the samples was left to cure within grips for 1 day and then outside the grips for 2 days for better adhesion. This combination was later pulled in tension in a MTS 810

tensile testing machine at a crosshead speed of 0.2 mm/min. The load at which failure occurred in the coin sample was recorded and the tensile bond strength was calculated. Figure 17 shows the assembly of coin samples and the rods before gluing, and the sample preparation kit and the curing procedure. Although this test provided bond strength that could be directly compared with the tensile strength of the base material, the test suffered from a limitation on the strength it could measure as this was restricted by the strength of the glue used to 40 MPa.

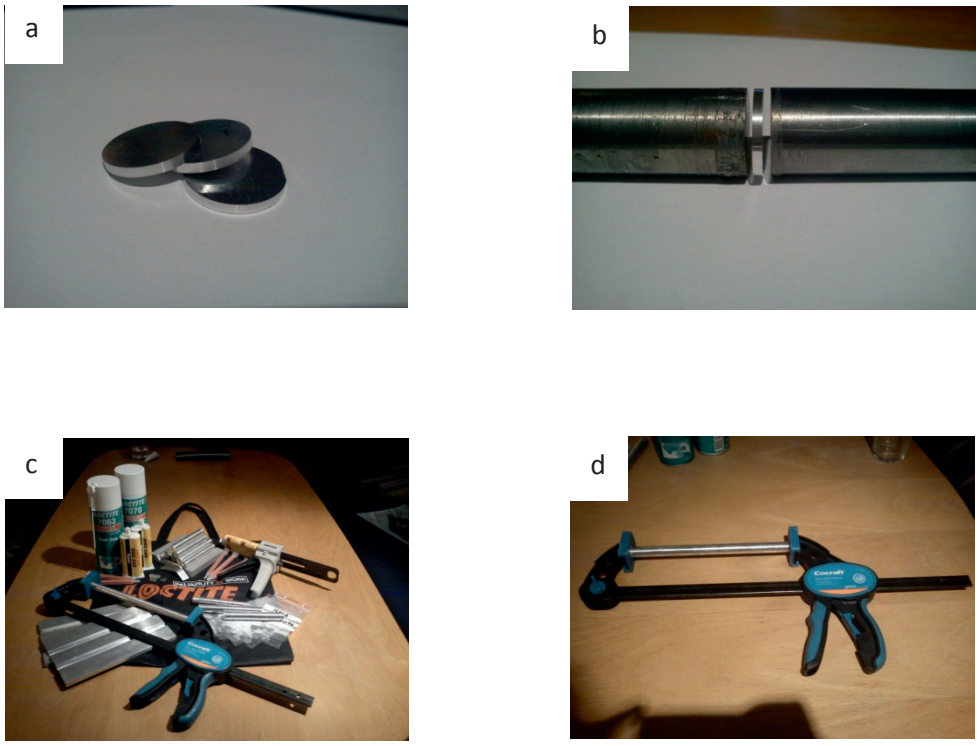

Fig.17. Sample preparation for the tensile bond strength test a) disc samples b) disc samples positioned between rods c) glue kit d) disc sample glued to rods curing under pressure

4.3. MATERIALS CHARACTERIZATION

4.3.1. SCANNING ELECTRON MICROSCOPY

Scanning electron microscopy makes use of interactions between a high energy electron beam and a specimen to obtain topographic and microstructural information from the specimen. When an accelerated beam of electrons is impinged upon the prepared surface of the specimen, a variety of signals are produced. These include, secondary electrons, backscattered electrons, X rays, transmitted electrons, cathodoluminescence and induced current in the specimen. Secondary electrons can be generally used for imaging and observation of topographical features on the surface and backscattered electron can be used for atomic number contrast and phase contrast [53]. Moreover, diffraction of the backscattered electrons can be used for investigating the local misorientations by using the EBSD (electron Back-Scatter Diffraction) technique, a schematic of which is shown in Fig.18.

Secondary electron imaging has been used to observe topographic features on the parted coin samples after the tensile bond strength test. The parted surfaces were observed in a Carl Zeiss - Ultra 55 field emission scanning electron microscope (FESEM). Stretch lips corresponding to failure in the regions that were originally bonded, un-bonded regions, cracks and deformed remains of previous wire brush marks were observed on these parted surfaces to characterize the bonded interface.

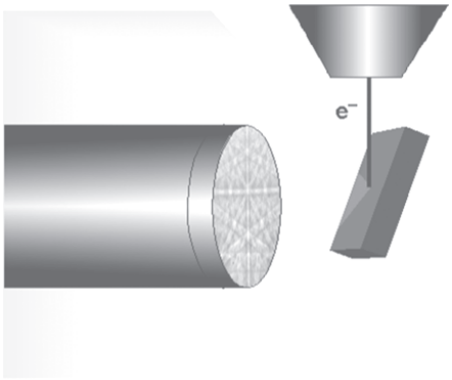

Fig.18. Schematic Electron backscatter diffraction technique

EBSD has been used in this work to investigate misorientations and to obtain grain boundary maps on deformed and annealed AA3103 samples. The preparation of the sample for this type of investigation involved mechanical grinding upto ASTM mesh 2400 followed by mechanical polishing with 3 μm and 1 μm diamond paste. This was followed by electro- polishing in a Struers LectroPol machine with a solution of 20 % Phosphoric acid and 80 % ethanol cooled to -25 °C at 20 V for 12 seconds.

EBSD analysis was carried out in a Hitachi SU6600 FESEM equipped with a NorDiff CD200 EBSD detector in addition to conventional detectors for secondary and backscattered electrons. The low angle grain boundary (LAGB) maps were obtained from scans over areas 15 μm X 15 μm with a step size of 50 nm in the rolling direction (RD) – normal direction (ND) plane. For better statistics, five scans were done for each case. All the scans were restricted to the center portion of the sample thickness so that inhomogeneity due to rolling induced shear stresses near

the surface was eliminated. The pattern data was collected and analyzed using the TSL OIM Data Collection 6 software and for post-processing TSL OIM Analysis 6 was used. Misorientation data was collected over a larger area of 175 μm X 225 μm with a step size of 0.5 μm in the RD – ND plane. Since the quality of diffraction patterns became poorer with increasing strain, this analysis was restricted to strain levels up to 2.3 in cold rolled AA3103. Microstructural features of severely cold rolled and ARB AA3103 could not be investigated using EBSD. This was one major limitation of using EBSD analysis in this work.

The details of the microstructure in the dissimilar ARB combinations were also observed in the secondary electron imaging mode. Contrast was obtained between the heavy and the light phases based on the difference in their ability to emit secondary electrons. Consequently, the heavy elements always appeared bright in these images. Thickness refinement, structural changes leading to shearing, necking and parting of the hard phase in the soft matrix and the structural changes in the soft phase have been captured using these images.

In the case of warm ARB'ed AA3103/Cu combinations, electropolishing for final surface preparation could not be used because an electrolyte that could work on both the materials was not available. Consequently ion milling was used for the final stage of surface preparation. After mechanical grinding and polishing as described before, the samples were subjected to milling in a Hitachi IM3000 flat ion milling system at 3kV for 45 minutes and the EBSD analysis was performed as described above. EBSD analysis was restricted to the Cu layer as only structural features in the hard layer were of interest. Scans were made on Cu layer at the center

of the sample thickness in the RD – ND plane over an area of approximately 45 μm X 40 μm with a step size of 0.1 μm.

4.3.2. TRANSMISSION ELECTRON MICROSCOPY

Transmission electron microscopy (TEM) has been used in this work to observe microstructural features in the AA3103 specimens after the low temperature annealing. TEM basically uses a focused beam of electrons accelerated to a high potential to probe an electron transparent specimen i.e a sample that is thin enough to transmit electrons through it. Transmitted and diffracted electrons contain information about the crystal structure of the region being analyzed. Since precipitates have preferred orientations in the matrix, the sample may be tilted so that the electron beam impinges it at specific angles, thus enabling better observation in different orientations.

The analysis was carried out in the longitudinal section of the samples containing the transverse direction (TD) and the rolling direction (RD) of the deformed strips. Thin foils were prepared from the strips by twin jet electro polishing in a solution of 33.3 % nitric acid in methanol at -25 °C and 15 V. The foils were examined on a Philips CM 30 microscope with a LaB_6 filament at 150 kV with the beam along the normal direction (ND).

4.3.3. ELECTRICAL CONDUCTIVITY

In AA3XXX alloys, it has been reported that elements in solid solution like Si & Cu have a much less influence on the electrical conductivity than Mn. Also, most of the Fe is reported to form intermetallic particles [54]. Consequently, electrical conductivity can be used to estimate the

content of Mn in solid solution and also trace changes in Mn content during different heat treatments. Electrical conductivity measurements have been extensively used to study changes in Mn content in solid solution in AA3103 alloys subjected to deformation and annealing. Also, conductivity measurements during the isothermal aging of deformed AA3103 alloy have been used to observe precipitation / clustering events during the heat treatment process. All the conductivity measurements have been performed using Foerster Sigmatest sigmascope at room temperature.

4.3.4. DIFFERENTIAL SCANNING CALORIMETRY

Calorimetry is a thermal analysis technique where the energy changes in a sample are measured as a function of temperature or time. When these measurements on a sample are made relative to a reference, the technique is called Differential Scanning Calorimetry (DSC). DSC has been widely used to analyze precipitation reactions in aluminium alloys [55, 56] and also for measurements of stored energy in nanostructure materials produced by top-down approach [57]. The technique is simple and transformation events can be easily captured by observation of endothermic or exothermic effects. Further, it proves to be a reliable alternative for precise estimation of recovery and recrystallization temperatures during softening heat treatments.

DSC has been used in this work to observe the heat changes occurring in severely deformed AA3103 alloy during heat treatments at low temperature. The DSC scans were carried out on a Sensys DSC setup from 30 ºC to 550 ºC at a low heating rate of 10 °C/ min in order to capture small heat changes. Helium atmosphere was used for better heat

transfer and sensitivity. Another reason for maintaining such a slow heating rate was to simulate conditions fairly similar to the low temperature heat treatments used in the hardening on annealing experiments.

4.3.5. TEXTURE

Rolled sheet materials acquire certain preferred crystallographic orientations by virtue of the deformation process and these preferred orientations can be represented by pole figures obtained by texture measurements on X ray goniometers. While the deformation step results in characteristic textures of its own, microstructural changes during the softening processes, especially recrystallization causes significant changes in the deformation textures resulting in recrystallization textures.

The back reflection method is the most common method for macro texture determination. Here, a flat specimen is mounted on a two circle goniometer - that can simultaneously rotate the sample about two orthogonal axes as shown in Fig.19.

Incident X ray beams from a source undergo Bragg diffraction at specific planes depending on the angles of tilt and the diffracted intensity is measured at the counter. A systematic rotation and tilt of the sample enables diffraction intensities from a certain volume to be collected and the pole figure is developed and the ODF can be obtained by deconvoluting the data.

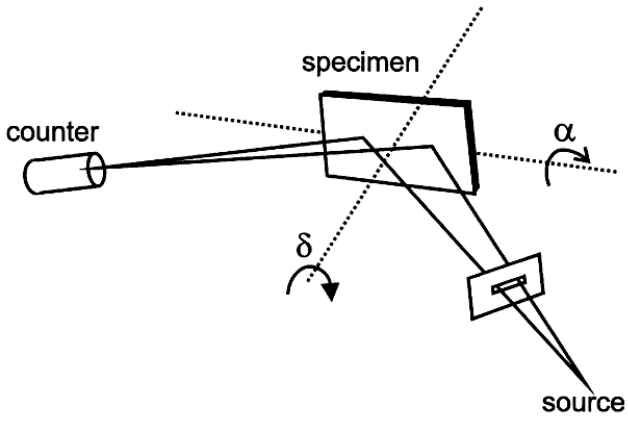

Fig.19. Schematic representation of the reflection method for determination of macro texture [58]

In this work, the texture goniometer has been used to measure possible changes in the macrotexture after subjecting cold rolled AA3103 samples to a low temperature annealing treatment. This was mainly done to observe if the heat treatments were causing texture changes and hence contributing to the hardening on annealing behavior.

4.4. DEFORMATION SIMULATIONS USING DEFORM 2D

Simulation of deformation processes on the computer is an ideal alternative to expensive and time consuming experiments. Simulations reduce the need for actual trials and redesign of tools and processes thereby facilitating virtual experimentation with reduced costs. Deformation simulation is mostly done using finite element method (FEM). A number of open source and commercial finite element software packages are available for such simulations. These could be general purpose FEM codes or packages tailored specifically for deformation

simulations. DEFORM is one such FEM package tailored specifically for deformation modeling and simulation.

Deform 2D package is generally used for modeling plane strain deformation in 2 dimensions as in the case of rolling and compression. The general process involves defining the geometry and the material of the work piece followed by simulation of each process step that is applied. This is accomplished by designing the process sequence as presented below

1) Process definition : - definition of starting work piece geometry, final part geometry, work piece material, tool geometry, tool progressions and processing conditions
2) Data : - collection of material data, data on process conditions
3) Building up the problem in DEFORM :- object description, material description, definition of inter-object relations and control parameters for the simulation
4) Simulation
5) Review of results
6) Iteration of simulation for each processing step

In DEFORM 2D, work piece geometry, material data and process conditions are fed into the pre-processor to build up the problem. The data is submitted for simulation to the simulation engine and the post-processor is used to analyze and review the deformation simulation.

In this work, deformation of dissimilar metal laminates has been studied by finite element analysis using the commercial FEM package DEFORM 2D. As a simple case, plane strain compression simulations with sticking

condition between alternate AA3003 and C10100 layers were used to examine macrostructural changes. It was ensured that the materials chosen from the DEFORM library were close to the actual material used in experiments. The models used for simulation are illustrated in Fig.20. Parameters investigated were the effective strain, strain rate and the stress on different layers. The model for plane strain compression was meshed with two dimensional quadratic elements with four nodes each. It was ensured that a minimum of four elements was available at all times in the thickness of a layer and the element size ratio (ratio of the largest to the smallest element) was maintained at 3. The model was deformed through displacements in the thickness direction and a total of 8000 elements per layer were used to capture the thickness refinement.

In addition to plane strain compression simulations, simulations of ARB experiments have also been attempted to precisely examine the deformation behavior of the multi-layer material in roll bonding conditions. The model for ARB was meshed with two dimensional quadratic elements with four nodes each. It was ensured that a minimum of four elements was available at all times in the thickness of a layer and the element size ratio (ratio of the largest to the smallest element) was maintained at 3. The model was deformed through displacements in the thickness direction and a total of 4000 elements per layer were used to capture the thickness refinement. A 9–layer model similar to the one used in plane strain compression simulations was used in this case also. The model illustrated in Fig.20.b was deformed by rolling with a thickness reduction of 50 % and the refinement in the thickness was mainly observed.

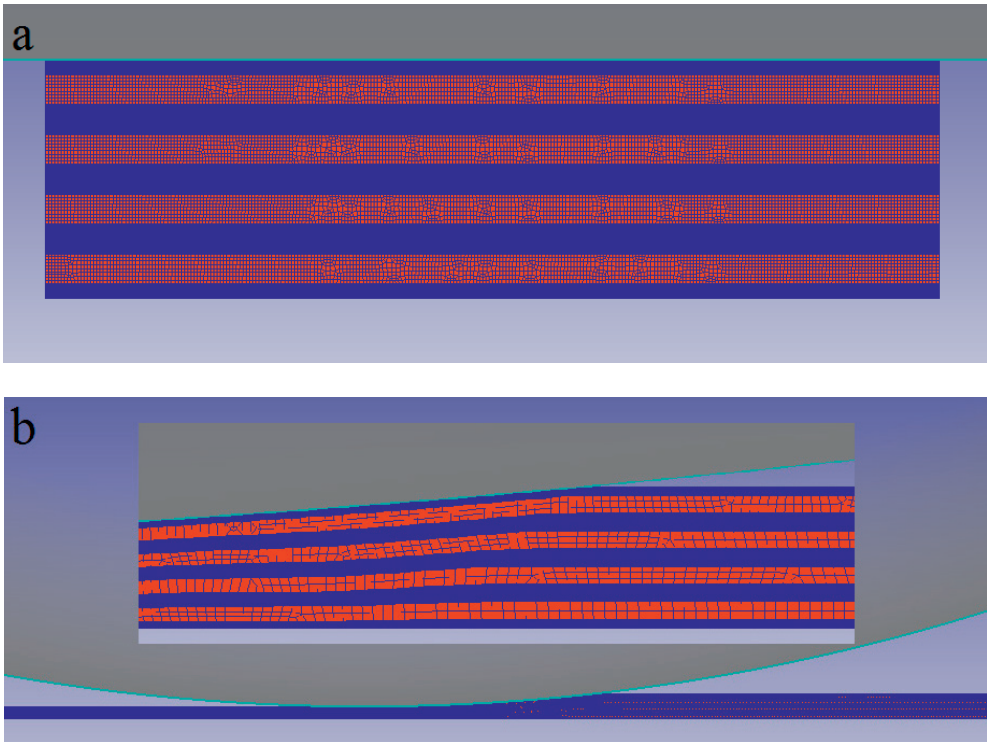

Fig.20. Model used for simulation of a) plane strain compression b)ARB of dissimilar material combination in DEFORM 2D (inset showing the layers entering the roll gap). AA3003 layers are shown in blue and Cu layers are shown in red.

5. SUMMARY

The broad scope of this work was to develop ARB process for development of new lightweight structural materials and also explore property improvements by nano-structuring and post processing heat treatments. Accordingly, different objectives were set and the outcomes of the work are presented as three independent articles published in / submitted to international scientific journals.

5.1. Tensile bond strength of cold roll bonded aluminium sheets

In this article, the objective of obtaining a better understanding of bonding at the interface is pursued by development of a new bond strength test in the tensile mode. Conventional bond strength test methods like the reverse bend test, peel test and shear test do not give a strength that can be directly compared with the tensile strength of the material. Also, the parted surfaces after these tests cannot be really examined to understand the bonding mechanism Hence, the need for an ideal testing method to assess the bond strength in tension which could provide parted surfaces with observable features was recognised and the tensile bond strength test was developed. In the tensile bond strength test, the roll bonded specimens were ripped open in a direction normal to the roll bonded interface by using long rods stuck to the opposite faces using an epoxy adhesive. The strength measured at failure of the interface thus gave a direct measure of the strength of the bond in tensile mode. The tensile bond strength test was performed on roll bonded strips of AA1200 and AA3103 alloy in two different tempers – ‘O’ and ‘H 19’. Additionally, in all the four cases, the bond strength was measured as a function of increasing rolling reduction. The results indicated that the

tensile bond strength test can be successfully used for testing bond strength up to 40 MPa limited by the strength of the glue. The method provides results that can be directly compared with the tensile strength of materials making design and material selection easy in soft alloys. Moreover, bond initiation and bond development stages in roll bonding can be directly studied using this test because it is sensitive to low bond strengths. Results show that the increase in bond strength with increased thickness reduction is higher in AA1200 when compared to AA3103 in both the temper conditions. The work also highlights the importance of reviewing the conceptual idea of a fixed threshold deformation for roll bonding as bond initiation and formation progressively occur over a broad range of deformations.

5.2. Hardening on annealing in cold rolled AA3103 strips

This article deals with the influence of post deformation heat treatments on the mechanical properties of materials deformed both by cold rolling and accumulative roll bonding. A series of low temperature annealing treatments above 150°C is reported to cause an increase in the strength of AA3103 alloy over a broad range of deformation levels achieved by cold rolling and accumulative roll bonding. The hardening on annealing behavior starts showing up after a deformation level of 1.7. The contribution of the classical dislocation source limitation mechanism for hardening on annealing is discussed but no softening is observed on a small deformation subsequent to the annealing process. Further, at low strains where closely spaced high angle grain boundaries are not available, sharpening of low angle grain boundaries is probed as an alternate mechanism for dislocation annihilation and hardening on

annealing. Homogenization is not observed to influence the extent of hardening on annealing in any way and conductivity measurements during isothermal annealing of a deformed AA3103 do not reveal any peaks indicating that there are no changes in the content of Mn in solid solution during these low temperature annealing treatments. DSC heat flow curves of the severely deformed AA3103 alloy show exothermic effects in the temperature range near those used in the low temperature annealing experiments indicating that some precipitation or clustering events were occurring. The probability of Si precipitation is also discussed but, the increase in the strength levels achieved only by precipitation of Si seems unrealistic. Further, model alloys with only Si in solid solution do not reveal any hardening when subjected to similar low temperature annealing experiments indicating that Si alone cannot cause this behavior. TEM investigation reveals precipitates in deformed AA3103 alloy annealed for long times at 225°C. It is concluded that hardening on annealing is observed only when alloying element Si is present along with other alloying elements like Mn or Fe in cold rolled AA3103 alloy. It is suggested that cluster formation by the diffusion of Si to the vicinity of other alloying elements could be the cause of hardening on annealing in AA3103 alloys.

5.3. Layer continuity in accumulative roll bonding of dissimilar material combinations

An investigation of the instability in the hard layer in accumulative roll bonding of dissimilar material combinations is presented in this article. AA3103 alloy was paired with commercial pure Cu strips and CuZn20 brass strips of certain thicknesses so that the ratio of the hard and soft

phases was equal. Cold ARB of multilayer metal composites was successfully performed up to 17 layers by 4 passes of Al and brass and up to 33 layers with 5 passes of Al and Cu in alternating layers. Further passes of cold ARB were prevented by severe flow instabilities with disintegration of the hard layers and cracking of the composite. At 350°C, 6 passes of ARB was performed to yield 64 Al and Cu layers. Macrostructural changes with increasing deformation were studied both in the Rolling Direction – Normal Direction (RD-ND) and the Transverse Direction – Normal Direction (TD-ND) sections and the strain levels at which the hard layers develop instabilities are observed. The influence of layer instability on mechanical properties was investigated by tensile tests and three point bend tests. Microstructural investigation by EBSD reveals shear bands in the hard Cu layer subjected to hot ARB. Numerical simulations of plane strain compression and ARB using the commercial finite element software DEFORM 2D were used for investigating the instability mechanism. The simulations showed that the instability mode is a zig-zag instability, where crossing 45° shear bands form and the result is a sinusoidal type of bending of the strongest layer by the opposite crossing shear bands. The zig-zag instability initially makes the strong layer more elongated and hence uniformly thinner as compared to the earlier assumptions of localized necking. Analytical estimates and explanations proposed earlier for necking in the hard layer are found not to be applicable and an onset of the zig-zag form of instability with the strong layers experiencing increased periodic thinning and bending is proposed as the mechanism. It is also suggested that layer control in these metallic multilayers might be possible by careful selection and control of the strength ratio and work hardening of the metal layers.

6. CONCLUDING REMARKS

In this section, general conclusions about the applicability of the tensile bond strength test to assess bonding properties in roll bonded materials are presented. Some remarks about the mechanisms governing increase in the tensile strength of deformed AA3103 by post-deformation heat treatments are made. Results of the study on instability in the hard layer in ARB of dissimilar material combinations are also presented.

The tensile bond strength test can be successfully applied at low rolling reductions to assess the initiation and development of bonding with the maximum strength tested being limited by the strength of the glue used. Additionally, deformation prior to roll bonding is found to have a positive influence on the bond strength in the tension mode. The need for reviewing the concept of a fixed threshold limit for bond formation in roll bonding is recognized from the fact that the bond strength gradually increases with increasing rolling reductions around threshold deformation limits.

The belief that severe deformation is a prerequisite for exhibiting hardening on annealing (HOA) is disproved in the article on hardening on annealing in AA3103 alloys. HOA is observed not only in AA3103 alloy severely deformed by ARB but also when the alloy is deformed to strains as low as 1.7 by cold rolling. The phenomenon requires a minimum strain and increases in magnitude with increasing rolling strains. For the cases of severe plastic deformation obtained by ARB the explanation of HOA by dislocation source limitation cannot be ignored, but the same explanation may not apply to the lowest strain of 1.7 where HOA occurred. Furthermore, the HOA was not removed by a subsequent 15%

rolling reduction, strongly indicating that dislocation source limitation is not causing the phenomena in AA3103. It is concluded that Mn plays a major role, because HOA was not observed in an Al-Si alloy that had almost the same composition as AA3103 but without Mn. However, in AA3103 the HOA was observed at a comparable extent for all the cases including an as-cast AA3103 with considerable amounts of Si and Mn in solution, an "industrially" homogenized AA3103 and AA3103 subjected to a homogenization treatment removing most of the Si in solution. Since the variations of Si in solution did not influence the magnitude of HOA, it is likely that Si is not directly involved. Diffusion of Mn at 225°C during 10 minutes seems unlikely but dislocation core effects may play an important role in the diffusion of Si towards other elements. Thus, formation of solute clusters or precipitation of very small particles seems likely. It is concluded that the HOA behaviour in AA3103 cannot be fully explained by existing theories but more detailed investigations involving atom probe and atomistic simulations might provide insight and lead to an explanation of this behaviour.

Based on FEM simulations and ARB experiments involving AA3103/Cu and AA3103/Brass, a new mechanism is proposed to cause instability in ARB of dissimilar material combinations. Estimates about the onset of instability from simplified analytical solutions were found not to apply as the simplifying assumptions are considered not to be realistic. The observed instability mode was two-dimensional and two-dimensional FEM simulations were performed. The predicted onset and mode of instability were in good agreement with what was found for the cold ARB of Al and Cu. The simulations showed that the instability mode is a zig-zag instability, where crossing 45° shear bands form and the result is

a sinusoidal type of bending of the strongest layer by the opposite crossing shear bands. The zig-zag instability initially makes the strong layer more elongated and hence uniformly thinner as compared to the earlier assumptions of localized necking. Layer control to avoid or extend this type of instability, might be possible by careful selection and control of the processing sequence, stacking sequence, strength ratio and work hardening of the involved metal layers. An onset of the zig-zag form of instability with the strong layers experiencing increased periodic thinning and bending is proposed as the new mechanism for loss of continuity and failure in the hard layers.

7. OUTLOOK AND FURTHER WORK

The results of experimental work presented in the three papers and the discussions that followed open new avenues for further experiments. Some of the ideas that were considered feasible to explore and investigate further are presented here.

In the first article, an interesting observation about the rate of increase in bond strength with increasing deformation was observed. The strength of the base alloy had a significant influence on this behavior. It would however be more interesting to measure the fraction of the material bonded at the interface by microstructural observation and correlate the measured fraction with the bond strength. Further, contributions of the surface roughness after surface preparation to the effective area of contact between two surfaces and its influence on fraction bonded and strength would help get a better understanding of the bonding at the interface. The tensile bond strength test can also be extended further to dissimilar material combinations and the limits of testing can be stretched by using stronger glues.

Formation of clusters/precipitates of Si with other alloying elements like Mn or Fe is suggested to be the cause of hardening on annealing behavior in deformed AA3103 alloys. However, these clusters/precipitates have not been visualized or observed in high resolution microscopy. 3 Dimensional Atom Probe (3DAP) Tomography can be used to identify the presence of such clusters in AA3103 alloys and also characterize these clusters so that a better understanding of their contribution to hardening on annealing can be obtained. Further, quantification of individual contributions from clusters and dislocation source limitation

can be attempted. A better understanding of the HOA behavior would provide some insight into the converse softening on deformation mechanism. Optimization of process parameters based on these mechanisms could help in tailoring the properties of deformed materials to specific requirements. An optimized combination of a severe deformation step that can cause adiabatic heating sufficient to alter the interior dislocation structure and a subsequent small deformation step to restore the dislocation structure could possibly help increase the strength of the material beyond the limits achieved by conventional deformation processing.

In the third article, a new mechanism for formation of instabilities in the hard layer in ARB of dissimilar material combinations is proposed based on experimental observation and numerical simulations. Although the mechanism is found to operate in representative dissimilar material combinations of AA3103/Cu and AA3103/Brass, its applicability to other common combinations in industry would be interesting to investigate. Additionally, the effect of other parameters like processing temperature, hardness and thickness ratio of the hard and soft layers and the effect of processing / stacking sequence on the control of layer continuity requires comprehensive analysis. An understanding of such instability mechanisms and the influence of processing parameters on continuity of the layers would be of great help in developing tailored multi-layer materials out of a wide range of otherwise incompatible material combinations. Thus bulk synthesis of functionally graded materials, deformation induced synthesis and transformation of multilayer materials, solid state amorphization and mechanical alloying of different materials will become a lot easier and cost effective. Control of

intermetallic phases in warm processing of dissimilar material combinations and development of optimized dissimilar combinations to suit specific applications are other areas that need investigation.

8. REFERENCES

[1] J. Dings, European Federation for Transport and Environment, (2011).
[2] I.Polmear, Light Alloys;From traditional alloys to nanocrystals, Fourth ed., Butterworth-Heinemann, 2006.
[3] A. Falkenö, SAE International, 2006.
[4] R. Baboian, M. Karavolis, SAE International, 1993.
[5] J. Scheel, ISATA - Dusseldorf Trade Fair, 1994.
[6] A. Bhowmik, S. Biswas, S. Suwas, R.K. Ray, D. Bhattacharjee, Metallurgical and Materials Transactions A, 40 (2009) 2729-2742.
[7] Y. Saito, H. Utsunomiya, N. Tsuji, T. Sakai, Acta Materialia, 47 (1999) 579-583.
[8] R.Z. Valiev, N.A. Krasilnikov, N.K. Tsenev, Materials Science and Engineering: A, 137 (1991) 35-40.
[9] J.Richert, M.Richert, Aluminium, 62 (1986) 604-607.
[10] Z. Horita, D.J. Smith, M. Furukawa, M. Nemoto, R.Z. Valiev, T.G. Langdon, Journal of Materials Research, 11 (1996) 1880-1890.
[11] S.H. Lee, Y. Saito, N. Tsuji, H. Utsunomiya, T. Sakai, Scripta Materialia, 46 (2002) 281-285.
[12] X. Huang, N. Kamikawa, N. Hansen, Materials Science and Engineering: A, 493 (2008) 184-189.
[13] X. Huang, N. Hansen, N. Tsuji, Science, 312 (2006) 249-251.
[14] M.C. Chen, H.C. Hsieh, W. Wu, Journal of Alloys and Compounds, 416 (2006) 169-172.
[15] M. Eizadjou, A. Kazemi Talachi, H. Danesh Manesh, H. Shakur Shahabi, K. Janghorban, Composites Science and Technology, 68 (2008) 2003-2009.
[16] G. Min, J.-M. Lee, S.-B. Kang, H.-W. Kim, Materials Letters, 60 (2006) 3255-3259.
[17] L.R. Vaidyanath, M.G. Nicholas, D.R. Milner, British Welding Journal, 6 (1959) 13-28.
[18] M. Schlesinger, The Recycling Industry, Aluminum Recycling, CRC Press, 2006, pp. 163-170.

[19] J.E. Hatch, Aluminum: Properties and physical metallurgy, American Society for Metals, Metals Park, Ohio, 1984.
[20] Ø. Ryen, B. Holmedal, O. Nijs, E. Nes, E. Sjölander, H.-E. Ekström, Metallurgical and Materials Transactions A, 37 (2006) 1999-2006.
[21] N. Bay, C. Clemensen, O. Juelstorp, T. Wanheim, CIRP Annals - Manufacturing Technology, 34 (1985) 221-224.
[22] N.Bay, International Welding Journal, 62 (1983) 137-142.
[23] L.R. Vaidyanath, D.R. Milner, British Welding Journal, 7 (1960) 1-6.
[24] R. Jamaati, M.R. Toroghinejad, Materials Science and Engineering: A, 527 (2010) 2320-2326.
[25] M. Buchner, B. Buchner, B. Buchmayr, H. Kilian, F. Riemelmoser, International Journal of Material Forming, 1 (2008) 1279-1282.
[26] N. Tsuji, Y. Saito, S.H. Lee, Y. Minamino, Advanced Engineering Materials, 5 (2003) 338-344.
[27] Y. Saito, N. Tsuji, H. Utsunomiya, T. Sakai, R.G. Hong, Scripta Materialia, 39 (1998) 1221-1227.
[28] X. Huang, N. Tsuji, N. Hansen, Y. Minamino, Materials Science and Engineering: A, 340 (2003) 265-271.
[29] N. Kamikawa, T. Sakai, N. Tsuji, Acta Materialia, 55 (2007) 5873-5888.
[30] K. Kitazono, E. Sato, K. Kuribayashi, Scripta Materialia, 50 (2004) 495-498.
[31] Y. Koizumi, M. Ueyama, N. Tsuji, Y. Minamino, K.i. Ota, Journal of Alloys and Compounds, 355 (2003) 47-51.
[32] N. Kamikawa, N. Tsuji, Y. Minamino, Science and Technology of Advanced Materials, 5 (2004) 163.
[33] X. Huang, N. Kamikawa, N. Hansen, Materials Science and Engineering: A, 483-484 (2008) 102-104.
[34] D. Yang, P. Cizek, P. Hodgson, C.e. Wen, Scripta Materialia, 62 (2010) 321-324.
[35] J. McKeown, A. Misra, H. Kung, R.G. Hoagland, M. Nastasi, Scripta Materialia, 46 (2002) 593-598.
[36] A. Srivastava, K. Yu-Zhang, L. Kilian, Frig, J. rio, J. Rivory, Journal of Materials Science, 42 (2007) 185-190.

[37] V. Jindal, V.C. Srivastava, A. Das, R.N. Ghosh, Materials Letters, 60 (2006) 1758-1761.
[38] V.Jindal, V.C.Srivastava, R.N.Ghosh, Materials Science and Technology, 24 (2008) 798-802.
[39] S. Ohsaki, S. Kato, N. Tsuji, T. Ohkubo, K. Hono, Acta Materialia, 55 (2007) 2885-2895.
[40] P.J. Hsieh, Y.P. Hung, J.C. Huang, Scripta Materialia, 49 (2003) 173-178.
[41] C.M. Cepeda-Jiménez, R.C. Alderliesten, O.A. Ruano, F. Carreño, Composites Science and Technology, 69 (2009) 343-348.
[42] C.M. Cepeda-Jiménez, M. Pozuelo, J.M. García-Infanta, O.A. Ruano, F. Carreño, Metallurgical and Materials Transactions A, 40 (2009) 69-79.
[43] H.S. Liu, B. Zhang, G.P. Zhang, Scripta Materialia, 65 (2011) 891-894.
[44] F.Bordeaux, R.Yavari, Z.Metall, 81 (1990) 130 -135.
[45] R.J. Hebert, J.H. Perepezko, Scripta Materialia, 50 (2004) 807-812.
[46] J.-M. Lee, B.-R. Lee, S.-B. Kang, Materials Science and Engineering: A, 406 (2005) 95-101.
[47] A.G. Atkins, A.S. Weinstein, International Journal of Mechanical Sciences, 12 (1970) 641-657.
[48] S.L. Semiatin, H.R. Piehler, MTA, 10 (1979) 97-107.
[49] F. Bourdeaux, R. Yavari, Z. Metallkde, 81 (1990) 130.
[50] Y.-M. Hwang, H.-H. Hsu, H.-J. Lee, International Journal of Machine Tools and Manufacture, 36 (1996) 47-62.
[51] Ö. Yazar, T. Ediz, T. Öztürk, Acta Materialia, 53 (2005) 375-381.
[52] S.L. Semiatin, H.R. Piehler, MTA, 10 (1979) 85-96.
[53] J. Goldstein, D.E. Newbury, D.C. Joy, C.E. Lyman, P. Echlin, E. Lifshin, L. Sawyer, J.R. Michael, Scanning Electron Microscopy and X-ray Microanalysis, Springer, 2003.
[54] Y.J. Li, L. Arnberg, Acta Materialia, 51 (2003) 3415-3428.
[55] N. Gao, M.J. Starink, T.G. Langdon, Materials Science and Technology, 25 (2009) 687-698.
[56] M.J. Starink, A. Dion, Thermochimica Acta, 417 (2004) 5-11.
[57] A. Godfrey, Q. Liu, Scripta Materialia, 60 (2009) 1050-1055.

[58] F.J. Humphreys, M. Hatherly, Recrystallization and related annealing phenomena, 2 ed., Elsevier, Oxford, 2004.

Article 1

Nagaraj Vinayagam Govindaraj, Steinar Lauvdal, Bjørn Holmedal

Tensile bond strength of cold roll bonded aluminium sheets

Published in Journal of Materials Processing Technology

Volume 213, Issue 6, 2013, Pages 955-960

Is not included due to copyright

Article 2

Nagaraj Vinayagam Govindaraj, Ruben Bjørge, Bjørn Holmedal

Hardening on annealing in cold rolled AA3103 strips

Submitted to Metallurgical and Materials Transactions A

Is not included due to copyright

Article 3

Nagaraj Vinayagam Govindaraj, Jan Gaute Frydendahl, Bjørn Holmedal

Layer continuity in accumulative roll bonding of dissimilar material combinations

Under review in Materials and Design

LAYER CONTINUITY IN ACCUMULATIVE ROLL BONDING OF DISSIMILAR MATERIAL COMBINATIONS

Nagaraj Vinayagam Govindaraj, Jan Gaute Frydendahl, Bjørn Holmedal

Department of Materials Science and Engineering

Norwegian University of Science and Technology

7491, Trondheim

Norway

Abstract

Strips were made by accumulative roll bonding of up to 64 alternating layers of an AA3103 alloy and either commercial purity copper or CuZn20 brass as the second type of layer. With increasing number of accumulative roll bonding cycles the layered structure became unstable. Instability in the strongest layer observed by secondary electron micrographs and orientation imaging micrographs revealed shear bands through the strong layers. The influence of the layer instability on the mechanical properties was investigated by tensile tests and three point bending tests. Numerical simulations using the commercial finite element software DEFORM 2D were used for investigating the instability mechanism in deformation of the multilayers. It is argued that the earlier proposed explanations and analytical estimates of the necking in the hard layers due to internal stresses do not apply. Instead the onset of the instability is in the form of a zigzag-shear instability, where the layers experience periodic increased thinning and bending.

Keywords: Accumulative roll bonding, layer continuity, deformation simulation

1. Introduction

Metallic multilayers belong to a new class of materials where thin layers of the metal are combined together by some bonding process into a single structural unit to yield better properties. Multilayer metallic materials produced from dissimilar metal combinations combine the unique advantages of the different metals involved to make composites that have better properties than the individual metals. In addition, these multilayers are reported to exhibit unique mechanical, electrical and magnetic properties when the layer thickness reaches the nanometer regime [1].

Originally, most of these multilayer materials were produced by expensive and time-consuming bottom-up processes like vapour deposition or epitaxial growth [2, 3]. Unfortunately, these methods could not produce products on a very large scale or in significant quantities. With the development of new forming techniques like repeated folding and rolling or accumulative roll bonding (ARB), it has been possible to produce multilayer materials on a bulk scale in sizes suitable for structural or industrial use [1, 4, 5].

It has been reported that in metallic multilayers made from dissimilar metals the harder material necks and ruptures resulting in a dispersion of lamellae in the soft matrix [6, 7]. This type of behavior can produce composites that are suitable for certain dispersion strengthening applications, where layer continuity is not important, while most other applications benefits from layer continuity giving a good load re-distribution between the constituent layers. Layer continuity is important for conductivity applications too. Moreover, the improved fatigue strength and toughness of a multi-layer roll bonded material can be

exploited only when the layers are continuous [8]. If necking in the hard layer can be overcome, there is a potential for refining the thickness down to nano-scale [7].

Deformation of sandwich materials has been widely investigated and a number of deformation models have been developed to predict the flow behaviour of the different materials in plane strain compression and rolling [9-13]. The main focus has been on clad and sandwich rolling, but the models can be applied to understand the deformation behaviour of the hard layer in ARB of dissimilar materials also. Atkins and Weinstein [9] argued that in-plane stresses, that are compressive in the softer component and tensile in the harder component, develop to satisfy the yield conditions. Semiatin and Piehler [13] proposed that such tensile stresses in the harder component may cause unstable flow and failure.

When a neck forms in the hard layer in a multilayer composite made up of dissimilar materials, localized deformation and preferential strain hardening of the soft matrix occurs in the vicinity of this neck. In a tensile test the necking occurs as a competition between local work hardening in the neck and locally reduced sheet thickness. In plane strain compression the total sheet thickness follows the tool movement and multiple necking occurs periodically along the rolling direction with exchange of material flow between the necks. Deformability of the hard phase is reported to be the determining factor that controls multiple necking and layer continuity in this case [10]. The continuity of the hard layer in the roll bonded multi-layer metallic material thus depends to a great extent on the strength and work hardenability of the hard layer. In addition to the flow properties, the initial thickness ratio i.e. the ratio of

thickness of the hard phase to the total thickness of the stack before roll bonding also has a strong influence on the necking and rupture of the hard phase [7].

Bordeaux and Yavari [10] assumed that the Considere criterion for necking applies in deformation of multilayer composites for the hard layer, based on the logarithmic thickness strain in compression, which is obviously wrong. Plastic instability criteria for diffuse necking and local necking during sandwich sheet rolling have also been developed by Hwang et al. [11] to predict the occurrence of plastic instability during rolling of sandwich strips bonded initially. In this work, the occurrence of plastic instability for local necking is concluded to be dependent on the strain hardening exponent of the hard layer, whereas, that for diffuse necking is dependent on initial thickness ratio, strength coefficients and strain hardening exponents of both the hard and soft layer. Nowicke Jr. et al. [12] pointed out that the diffuse necking criterion suggested by Hwang et al. [11] is wrong. They found experimental evidence for that the instability can be delayed by increased amount of hard phase in the clad sheet or by the use of small radius rolls and concluded from hardness measurements and from finite elements simulations that increasing redundant shearing in the soft phase was causing this. However, their experimental results could not be predicted by the simple analyses by Semiatin and Piehler [13].

In this work, the problem of instability during accumulative roll bonding (ARB) of multilayers of AA3103 layers alternated with either Cu or alpha-Brass (CuZn20) layers is analysed. The ARB processing at room temperature and at a higher temperature and the experimental testing is

described in Section 2. Results from these experiments are presented in Section 3 and a simplified analytical stability analysis of the layers during ARB along with an introduction to the models used in finite element simulations are presented in Section 4. A short discussion comparing the experimental results with simulations and analytical solutions constitutes Section 5 before the conclusions in Section 6.

2. Experimental methods

Approximately 30 mm wide AA3103 strips were cold rolled to a thickness of 1 mm or 0.5 mm from a 20 mm thick billet cut from DC cast homogenized AA3103 material. These strips will henceforth be referred to as aluminium strips. 30 mm wide strips of commercial purity Cu or CuZn20 brass (Br) were cut from 1 mm thick sheets, which were in a soft, slightly cold rolled condition. With 50% rolling reduction proper metallic bonding between the aluminium and Cu or Br strips could not easily be achieved at room temperature, hence the first pass of rolling was always made in the hot condition. However, good bonding can be achieved between two aluminium surfaces even at room temperature. Hence a sandwich with two outermost layers of aluminium strips of half the thickness as either Cu or Br in the middle, were made by hot ARB in the first pass. This enabled subsequent ARB passes to be made in a cold condition with a one to one thickness ratio between the strong and the soft layers. For cases where the subsequent passes were by hot rolling, the bonding was good and a simpler stack of only two dissimilar strips could be made at the first pass.

The stacks were pre-heated to 350 °C and held at that temperature for 10 minutes in an air convection furnace and then subjected to warm roll

bonding in a 2 high rolling mill with roll diameter 205 mm. The thickness reduction was maintained to be a constant value of 50 % in each rolling pass and the roll bonding process was repeated up-to 6 cycles, either by subsequent warm or cold rolling passes. Precaution was adopted to complete the cold roll bonding cycles within 2 minutes of surface preparation. All the roll bonded samples were 200 mm in length and about 20 mm in width in the last pass due to the need of trimming the edges between the passes. The composites made by subsequent cold ARB will be denoted CARB.

Tensile samples parallel to the rolling direction (RD) were machined out of the roll bonded material according to the dimensions in Fig.1. The tensile tests were carried out with a 10 mm extensometer on a MTS 810 tensile testing set-up at a constant crosshead speed of 2 mm/min.

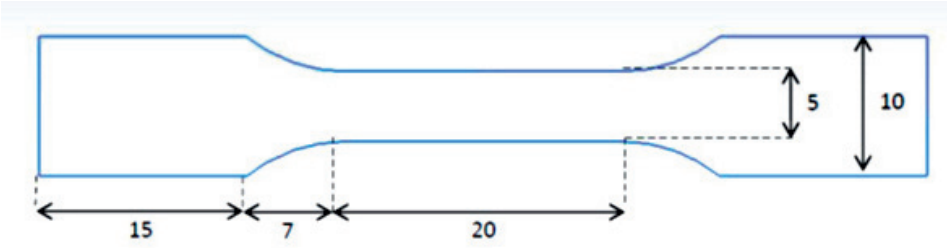

Fig.1. Specimen used for tensile testing (all dimensions are in mm)

Rectangular samples (40 mm long and 10 mm wide) were machined from the ARB strips for three point flexural testing. The samples were subjected to bending at a constant stroke rate of 2.4 mm/min up to a displacement of 8 mm, and the force and displacement were recorded.

The rolling direction - normal direction (RD-ND) and transverse direction - normal direction (TD-ND) cross sections of the ARB

specimens were observed in a Hitachi SU6600 scanning electron microscope (SEM) in the secondary electron imaging (SE) mode. The details of the microstructure were also evaluated by electron backscatter diffraction (EBSD) analysis on Cu layer at the center of the sample thickness in the RD – ND plane. The samples were subjected to ion milling after conventional mechanical surface preparation in a Hitachi IM 3000 flat milling system. A voltage of 3 kV was used for 45 minutes to mill off the surface layers of the deformed material. EBSD was carried out on a Hitachi SU 6600 FEGSEM equipped with a NORDIF UF1000 detector and the data analysis was carried out using TSL OIM 6.0 software. Scans were performed on the samples in the rolling direction (RD) – normal direction (ND) plane at the center of the thickness. Structural refinement and shear bands in the hard phase have been captured through the EBSD analysis.

3. Experimental results

Laminated metal strips were processed by ARB in cold and warm (about 350°C) conditions. The material flow and layer integrity was investigated by microscopy and are presented in Section 3.1. The mechanical properties of the ARB samples were tested by tensile tests and by three point bending tests, the results of which are shown in Section 3.2.

3.1 ARB of alternating layers

Secondary electron images from RD-ND and TD-ND sections of the maximum deformed specimens prepared are presented in Fig.2. For all the cold ARB specimens, a general observation in the microstructures is a wavy instability leading to fracturing and departing of the hard phase.

The instability in the hard phase is however almost absent in the TD-ND section when compared with the RD-ND section, indicating that the instability is two-dimensional.

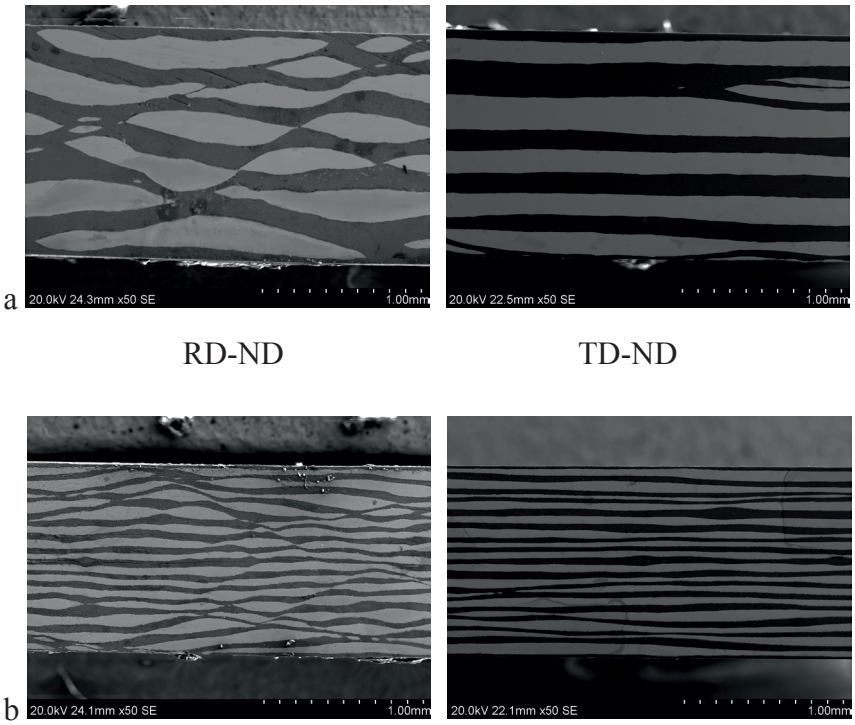

Fig.2.Secondary electron images of RD ND and TD ND sections of the maximum deformed ARB composite specimens: a) Cold ARB of Al and Br after 4 passes, b) cold ARB of Al and Cu after 5 passes

c 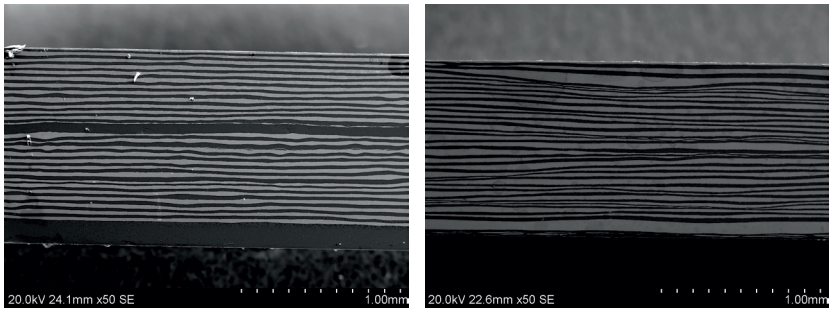

RD-ND TD-ND

d 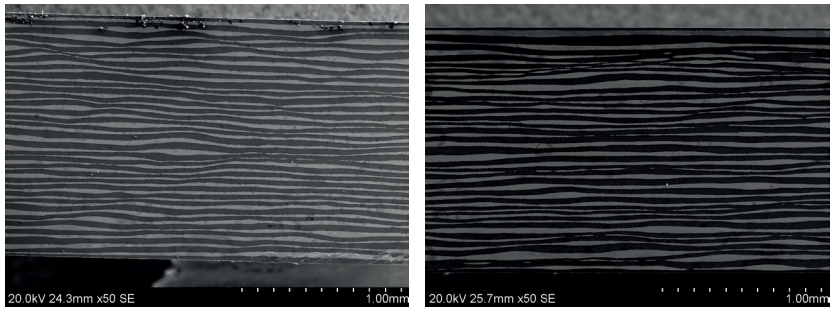

RD-ND TD-ND

Fig.2.Secondary electron images of RD-ND and TD-ND sections of the maximum deformed ARB composite specimens: c) warm ARB of Al and Cu after 6 passes, and d) warm ARB of Al and Cu based on the sandwich with two Al layers and one Cu layer, all of equal thickness, after 6 passes.

It can be observed in Fig.2a that after one warm and three cold ARB passes the hard Br phase is broken up and fragmented by 45° shear bands running through the layers and efficiently preventing further thickness reduction of the hard layers. The string-like structure must be a result of inhomogeneous deformation with multiple fractures in the transverse direction in the hard layers after 4 passes of ARB. Since the TD-ND sections show fracture to a small extent it is a two-dimensional instability

mode. It is to be noted that necking, fracturing and departing of the brass layers occurred simultaneously during the fourth pass of ARB and most of the necking sites are aligned at roughly 45° to the loading direction. Similar behaviour has been reported to occur already at the first pass of ARB of Al/Ni [5]. In both cases necking, fracture and departing occurred during the same cycle of ARB.

Cold ARB of Al and Cu on the other hand exhibits considerable thickness reduction in the Cu layer after five passes of ARB, as can be seen in Fig.2b. A two-dimensional layer instability with a wavelength comparable to the layer thickness can be observed in the RD-ND section, with only a weak variation with a considerable longer wavelength in the TD-ND section. Here again, the necking sites are roughly 45° to the loading direction but the elongation has been even more extensive than in the Al and Br samples.

Warm ARB of Al and Cu exhibits instabilities in the layers first after 6 passes with a corresponding higher thickness reduction of the hard layer before instability occurs, as shown in Fig.2c-d. The extent of instabilities is less severe than for the cold ARB cases. Note also that the instability mode is more three-dimensional with less difference between the extent of instabilities in the TD-ND and the RD-ND sections. However, ARB beyond 6 passes and investigation of the further layer refinement was not possible due to the edge cracks evolving during rolling.

It has been reported earlier by Lee et al.[7] that a higher initial thickness ratio between the soft and the hard layer gives earlier instability, and this was the case for the sandwich case with relatively thinner Cu layers,

which shows a more developed instability in Fig. 2d. It is interesting to note that the mode of instability in this case is more three-dimensional.

EBSD maps of the Cu layer after 4 passes of warm ARB of Al and Cu is presented in Fig.3. The ARB of the sandwich of three layers of unequal thicknesses was chosen, because instability in the hard layer occurred at the lowest deformation with the relatively thinner hard layer, and the warm deformed material allowed good diffraction conditions for EBSD. Shear bands can be observed as a prominent feature in the sample.

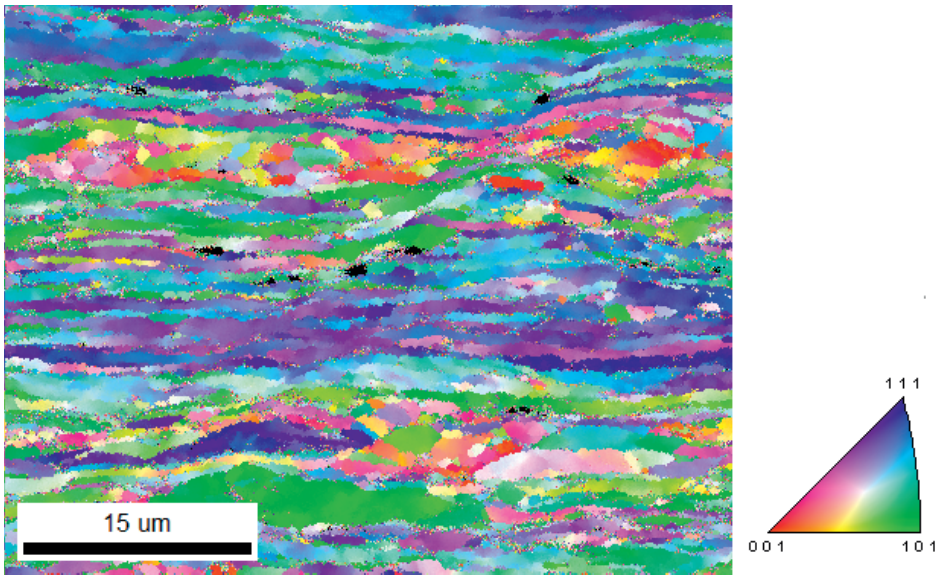

Fig.3.EBSD map from a Cu layer near the centre of the RD-ND section in a sample processed by four passes of warm ARB with Al layers half as thick as Cu layers.

3.2 Mechanical testing

Tensile properties of metal composites processed by various number of ARB passes are presented in Fig. 4. A general observation for all the cold

ARB specimens is that the strength increases with increasing number of ARB passes. A significant scatter in tensile values can be seen for multi-layer specimens when delamination occurs in some of the samples. It can be observed from Fig. 4a that cold ARB of Al and Br gives a high strength but a poor elongation already after one pass. The samples processed by several passes fail before the yield point is reached. Fig. 4b reveals that cold ARB of Al and Cu exhibits lower levels of strength but significant improved ductility as compared to the cold ARB of Al and Br. However, with three passes or more some samples fracture earlier. In the warm ARB condition shown in Fig.4c, the Al and Cu combination exhibits an increase in strength with increased number of ARB passes.

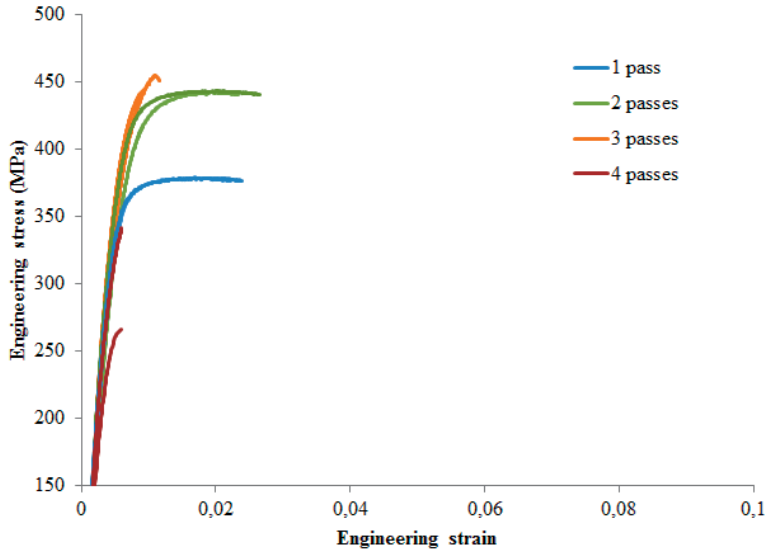

a

Fig.4. Tensile tests of composites with equal ratios of hard and soft phases: a) made by cold ARB of Al and Br layers after a warm first pass

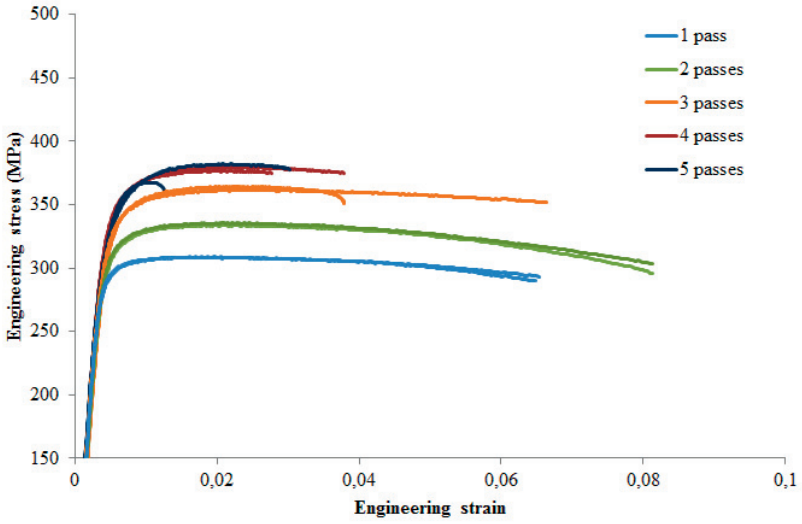

b

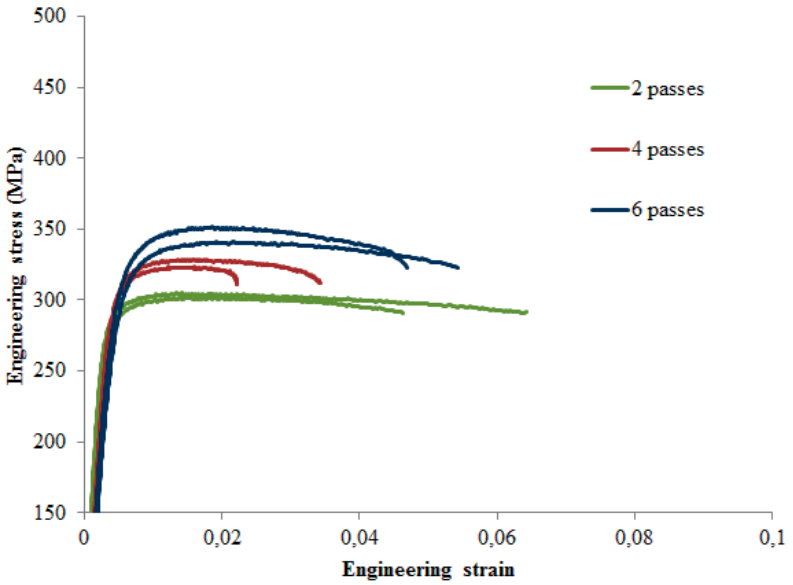

c

Fig.4. Tensile tests of composites with equal ratios of hard and soft phases: b) made by cold ARB of Al and Cu layers after a warm first pass, and c) made by warm ARB of Al and Cu layers after 2, 4 and 6 passes.

Results from the three-point flexural tests are presented in Fig.5 for cold ARB specimens. Both the force and displacement are normalized with respect to the sample thickness accounting for thickness variations, according to the formula:

$$\sigma_f = \frac{3PL}{2bd^2} \tag{1}$$

Here σ_f is the flexural tensile stress at the outer surface. The displacement is *l*, the measured force is *P*, *L* is the span between supporting rolls, *b* is the width of specimen, *d* is the thickness of specimen.

For both material combinations the flexural strength increases and the ductility decreases with increasing number of ARB passes. For the combination of Al and Br presented in Fig.5a, the sample subjected to 1 pass ARB shows a continuous strain hardening, whereas the sample after 2 passes shows a drop and rise in the load, characteristic of delamination, crack formation in the harder layer, crack arrest followed by plastic deformation and crack re-nucleation. The third pass sample exhibits a higher flexural strength and a very low ductility, and the fourth pass sample shows neither strength nor ductility.

Delamination and cracking of layers is evident already from the 1 pass with Al and Cu in Fig.5b, for which a slow and stepped curve lowering of the flexural strength followed by plateau after the load drop is interpreted as plastic deformation of the remaining material and crack re-nucleation. Such a slow and stepped drop after crack propagation can however not be observed in the samples subjected to larger number of ARB passes.

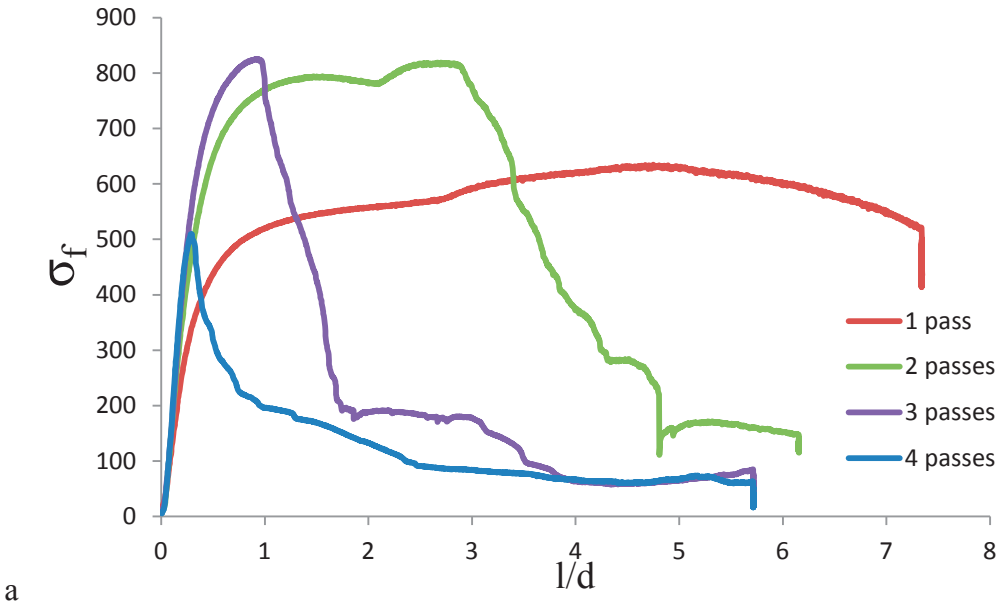

a

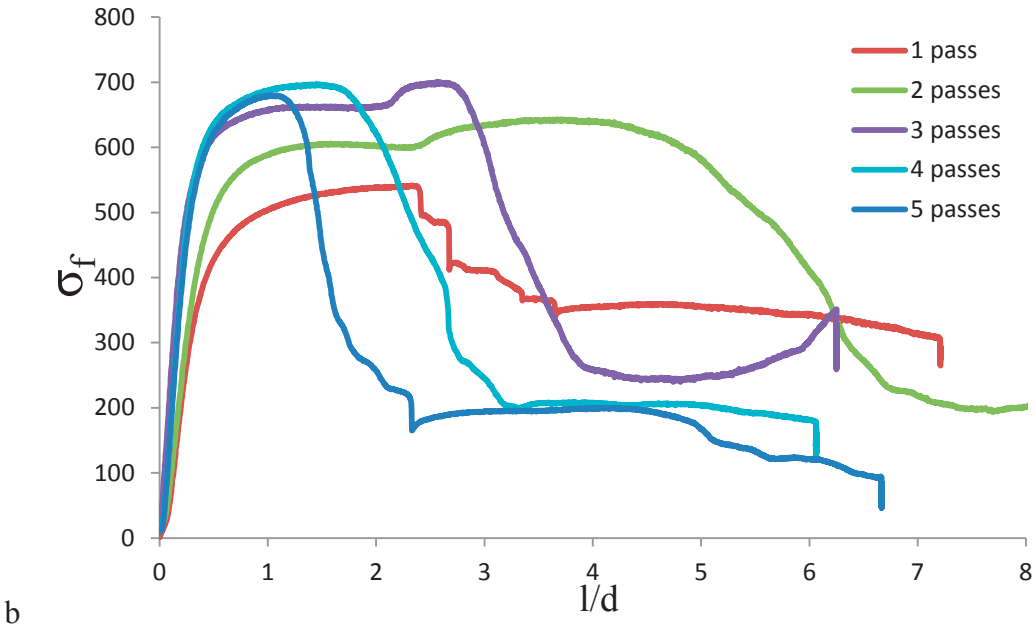

b

Fig.5. Flexural strength of cold ARB samples from 3 point bending tests of composites of: a) Al and Br and b) Al and Cu.

4. Stability analysis

At some point during ARB, the approximately uniform plane strain compression deformation mode of the layers becomes unstable. A simplified analytical solution can be found for the case of uniform plane strain compression of the layers, for which a simplified stability analysis can be performed. The validity of the simplifications is discussed and next the analytical results are contrasted to FEM simulations of this idealized case in Section 4.1, where the gradual onset of instability could be studied. The commercial finite element analysis package DEFORM 2D was used to analyse deformation and material flow. The cold deformation of aluminium and copper was chosen, for which a basically two-dimensional instability can be expected from the experimental ARB results. However, once the instability occurs, the simplified plane strain compression mode is no longer a good approximation for ARB. Hence a simulation of the rolling gap is performed in Section 4.3.

4.1 Analytical stability analysis

The geometry of the rolling of several layers is schematically shown in Fig.6. Alternating layers of soft (thickness t_S) and hard (thickness t_H) materials are rolled. Before the rolling pass the total thickness of the sandwich is t and fraction of the thickness occupied by the hard layers is f. Analytical solutions for rolling has been given by Atkins [9].

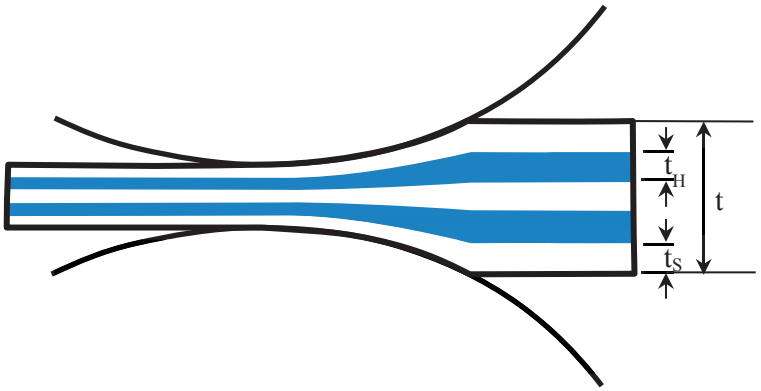

Fig.6. Multilayer rolling geometry of a sandwich strip of thickness t, with alternating soft and hard layers of thickness t_S and t_H , respectively.

The simplest approximation is plane-strain compression in the strip-normal direction with no friction between the tool and the outermost layer. A shear stress is required to transfer the internal stresses across the interfaces between the layers, but its contribution to the yield stress and also the shear components are neglected in the simplified analytical solution. For this simplified case a number of stability analyses have been proposed for clad materials [11-14]. These analyses can be extended to multilayers. While Steif [14] performed a bifurcation analyses, the approach of other analyses by Siematin and Pieler, Hwang et al. and Nowicke Jr. [11-13] was to assume a simplifying analogy to the stability of unconstrained strips in biaxial load. Only the major stresses are involved, where the major stress of each layer acts in the rolling direction. Since no force is applied in the rolling direction, the force balance becomes.

$$f\sigma_{1H} + (1-f)\sigma_{1S} = 0 \qquad (2)$$

Here σ_{1H} and σ_{1S} denotes the major stress in the hard layer and soft layers, respectively. The basic assumption is that the materials are approximated by a rigid plastic isotropic von Mises material.

$$\begin{aligned} F(\bar{\sigma}) &= \bar{\sigma} = \frac{\sqrt{2}}{2}\sqrt{(\sigma_1-\sigma_2)^2+(\sigma_2-\sigma_3)^2+(\sigma_1-\sigma_3)^2} \\ d\bar{\varepsilon} &= \sqrt{\tfrac{2}{3}\left(d\varepsilon_1^2+d\varepsilon_1^2+d\varepsilon_1^2\right)} \end{aligned} \tag{3}$$

It follows from the associated flow rule and no transverse elongation that

$$d\varepsilon_2 = d\lambda\frac{\partial F}{\partial \sigma_1} = \frac{d\lambda}{2\bar{\sigma}}(2\sigma_2-\sigma_1-\sigma_3) = 0 \tag{4}$$

Hence the plane strain von Mises yield function can be written

$$F = \bar{\sigma} = \sqrt{\tfrac{3}{2}}\left|\sigma_1-\sigma_3\right| \tag{5}$$

The strip normal pressure is equal through the layers

$$\sigma_{3H} = \sigma_{3S} \tag{6}$$

From Eq. (1)-(5) the simple analytical solution can be derived

$$\begin{aligned} \sigma_{3H} &= \sigma_{3S} = -\tfrac{2\sqrt{3}}{3}\left((1-f)R_S + fR_H\right) \\ \sigma_{1S} &= -\tfrac{2\sqrt{3}}{3}f\left(R_H-R_S\right) \\ \sigma_{1H} &= \tfrac{2\sqrt{3}}{3}(1-f)\left(R_H-R_S\right) \\ \sigma_{2S} &= -\tfrac{\sqrt{3}}{3}\left(R_S+2f\left(R_H-R_S\right)\right) \\ \sigma_{2H} &= -\tfrac{\sqrt{3}}{3}\left(2f\left(R_H-R_S\right)+2R_S-R_H\right) \end{aligned} \tag{7}$$

Here R_S and R_H are the flow stresses of the soft and hard layers respectively. This solution is independent of the hydrostatic pressure. Conveniently, by imposing a hydrostatic pressure $p = -\sigma_{3S} = -\sigma_{3H}$ the condition become plane stress, i.e. the layer interfaces are traction free.

$$\begin{aligned}
&\sigma'_{3H} = \sigma'_{3S} = 0 \\
&\sigma'_{1S} = \tfrac{2\sqrt{3}}{3} R_S \\
&\sigma'_{1H} = \tfrac{2\sqrt{3}}{3} R_H \\
&\sigma'_{2S} = \tfrac{\sqrt{3}}{3} R_S \\
&\sigma'_{2H} = \tfrac{\sqrt{3}}{3} R_H
\end{aligned} \qquad (8)$$

For each layer this setup is similar to the assumptions for stability analyses of necking of a strip in plane stress biaxial loading, provided that the constraint from the deformation of the soft layer can be neglected. Assuming that the induced shear flow and deformation in the soft layer requires a relatively low energy, Hills criterion for local necking and Swifts criterion for diffuse necking coincide. The criterion for instability is then

$$\begin{aligned}
&\frac{d\sigma'_{1H}}{d\varepsilon_1} = \sigma'_{1H} \\
&\frac{d\bar{\sigma}_H}{d\bar{\varepsilon}} = \tfrac{\sqrt{3}}{2} \bar{\sigma}_H
\end{aligned} \qquad (9)$$

This criterion is the same as obtained by Hwang et al. [11] for the case of local necking. However, their criterion for diffuse necking is wrong, as pointed out by Nowicke Jr. et al. [12]. Also, the criteria for local necking given by Siematin and Pieler and Nowicke Jr. [12, 13] can be incomprehensive. The instability occurs earlier than the maximum force

in the rolling direction in the hard layer. The instability estimate in Eq. (8) must be considered as a lowermost limit for instability to occur in the hard layers assuming the other layers are much softer. Given a hard material obeying a power law $R_H = K\bar{\varepsilon}^n$, the instability will occur at $\varepsilon_3 = -\varepsilon_1 = -\frac{\sqrt{3}}{2}\bar{\varepsilon} = -n$.

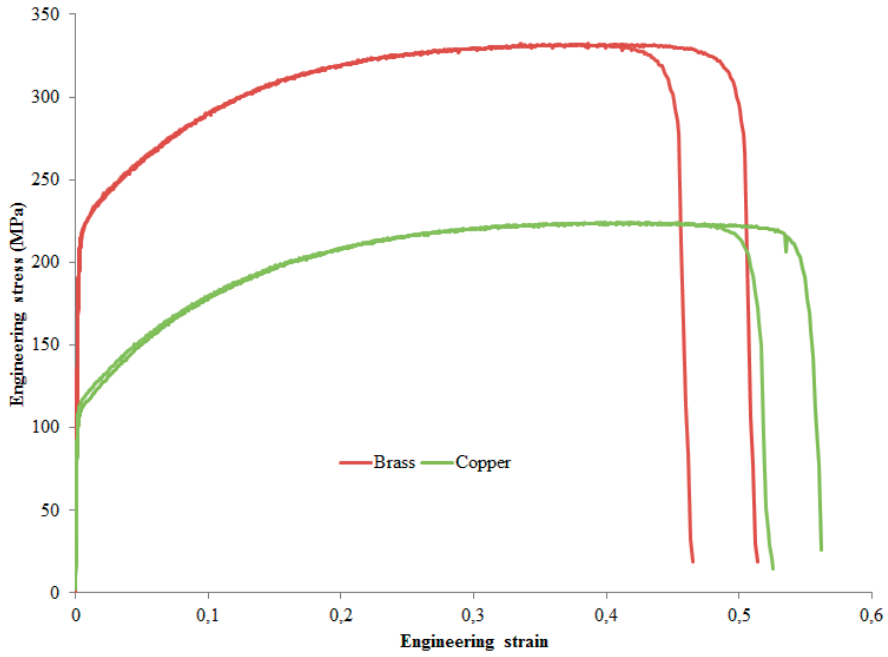

Fig.7. Engineering Stress strain curves of the harder materials used in ARB.

Material	σ_u	ε_u	K	n
Br	452	0.31	649.85	0.31
Cu	312	0.33	449.83	0.33
AA3103	253	0.02	273.58	0.02

Table 1. Tensile properties of the starting materials.

Tensile properties of the starting materials are presented in Table 1. The corresponding tensile curves in Fig.7 show considerable work hardening of these slightly pre-rolled Br and Cu strips. The work hardening is decreasing, and according to the simplified analytical stability analysis, estimates that instability in the hard layer would occur at strains still within the first pass of ARB with any of these two materials. However, observation by micrographs reveals that instabilities started occurring during the 4^{th} pass both for the combination Al and Br and for Al and Cu., i.e. after a total Von Mises strain larger than 2.4.

The simplifying assumptions made in most of the analytical stability analyses are not very realistic. The strip surface is constrained by that the layers above and below have to be deformed and by the horizontal tools at the outer layers and the volume of the stack being conserved in between. Local thinning of a groove in the transverse direction in the hard layer would require a corresponding thickening of the soft layers above and below. However, such a thickening would decrease the lengths of the two soft layers and a horizontal material flow would be required in the rolling direction, i.e. shear flow as observed in Fig 3.

4.2 FEM simulation of plane strain compression

A specimen corresponding to uniform plane strain deformation after three passes of ARB was modelled with 17 alternating layers of copper in aluminium, starting with a uniform von Mises strain equal to 2.4. Symmetry across the middle of the specimen was assumed. Due to symmetries only a quarter of the specimen was modelled, as illustrated in Fig. 8. Sticking condition was defined between the alternating layers. Both types of layers were assumed to behave as isotropic von Mises

materials. The layers in the model were meshed with two dimensional linear quadrilateral elements with four nodes each. It was assumed that after three passes of ARB the materials would have no work hardening, because saturation of the stress-strain curves occurs around these strains for both these materials. The yield stresses were assumed to be 450MPa for Cu and 300MPa for Al. An attempt was made to run the simulation with a 50MPa stage IV slope of the stress strain curve. However, instability did only occur for the case without work hardening, and this is the case that will be discussed below.

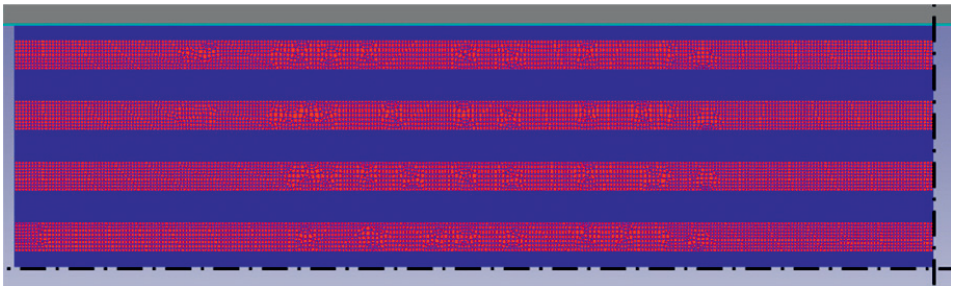

Fig.8. Multi-layer Al-Cu model for FEM simulation of plane strain compression. The boundaries on the lower and right edges are symmetry boundaries indicating that only a quarter of the sample was modelled.

At first the layers deform uniformly, then after a von Mises strain of about 2.5 instability evolved gradually. Strain rate plots from DEFORM 2D simulations are shown in Fig.9 and reveal an alternating pattern of strain rates during deformation subsequent to the onset of instability. These patterns are similar to the crossed shear bands observed in the micrographs in Fig.5, appearing mostly at 45° to the deformation direction. Instabilities could be arising in these regions of deformation

triggered by the difference in flow properties of the hard and the soft layer. A manifestation of such instabilities extending into the hard layer can be the shear bands observed in Fig. 3. Instabilities in the copper layer started showing up in this simulation when the total strain reached a value of around 2.7 and became more pronounced with increasing strain as illustrated by Fig.10b, showing the layers at a strain of 3.1.

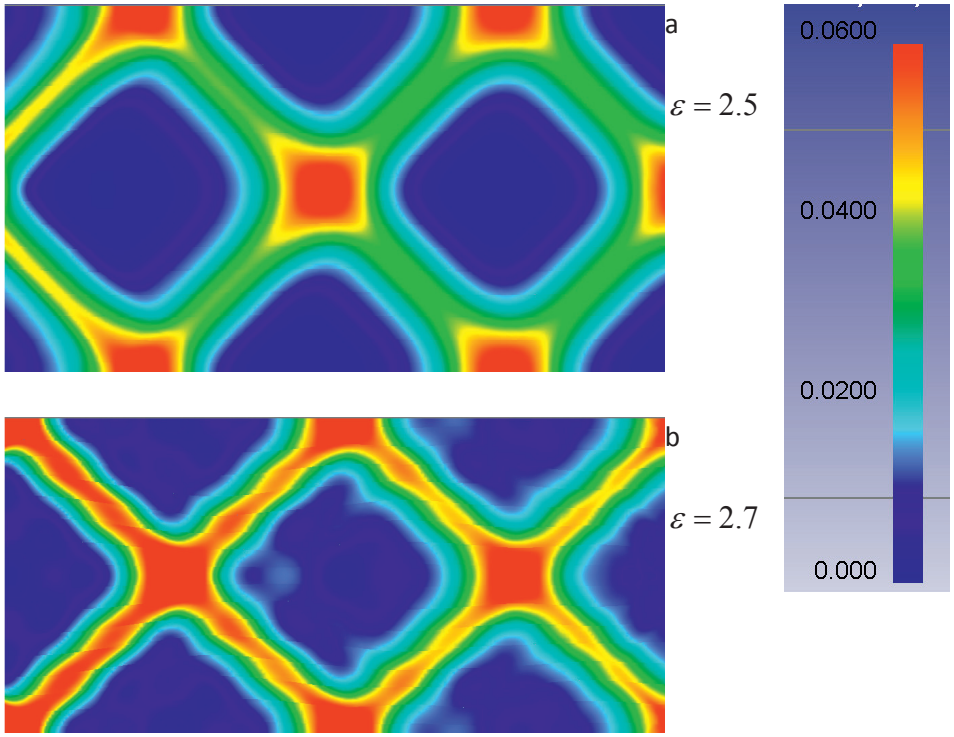

Fig.9. Effective strain rate plots on Al/Cu stack showing alternating patterns in a compression simulation of Al and Cu multilayers at strains of a) 2.5 b) 2.7

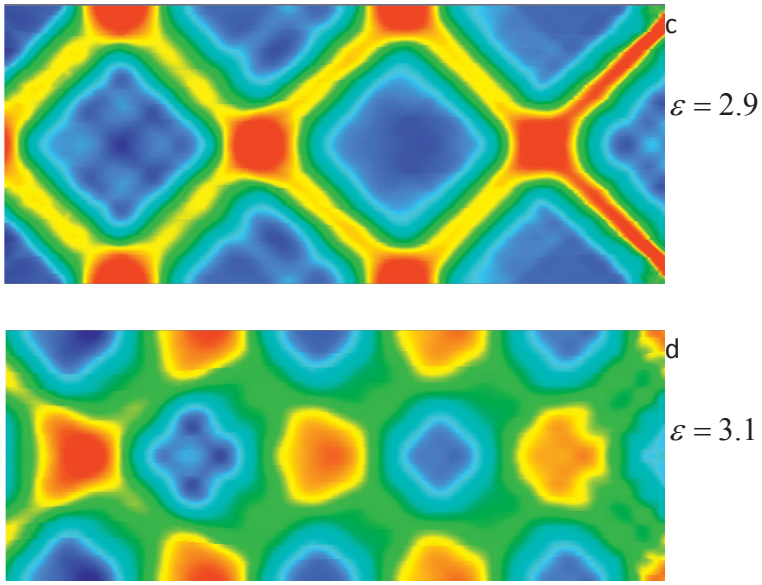

Fig.9. Effective strain rate plots on Al/Cu stack showing alternating patterns in a compression simulation of Al and Cu multilayers at strains of c) 2.9 d) 3.1. The Cu layers start to become wavy at a strain of around 2.7.

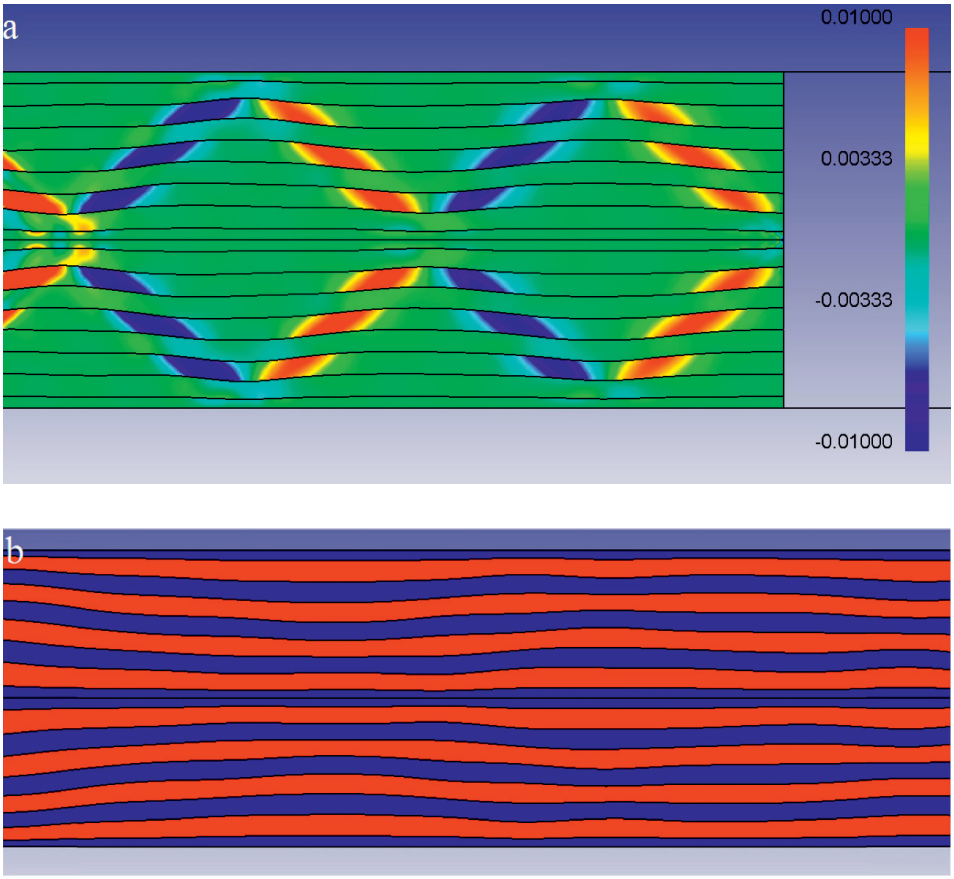

Fig.10.a) Shear strain rate plots showing alternating shear patterns in the soft layers in a compression simulation of Al and Cu multilayers at a strain of about 2.6. b) Wavy pattern in Al and Cu multilayers compressed to a strain of 3.1 indicating zigzag type of instability, Al layers are shown in blue and Cu layers are shown in red

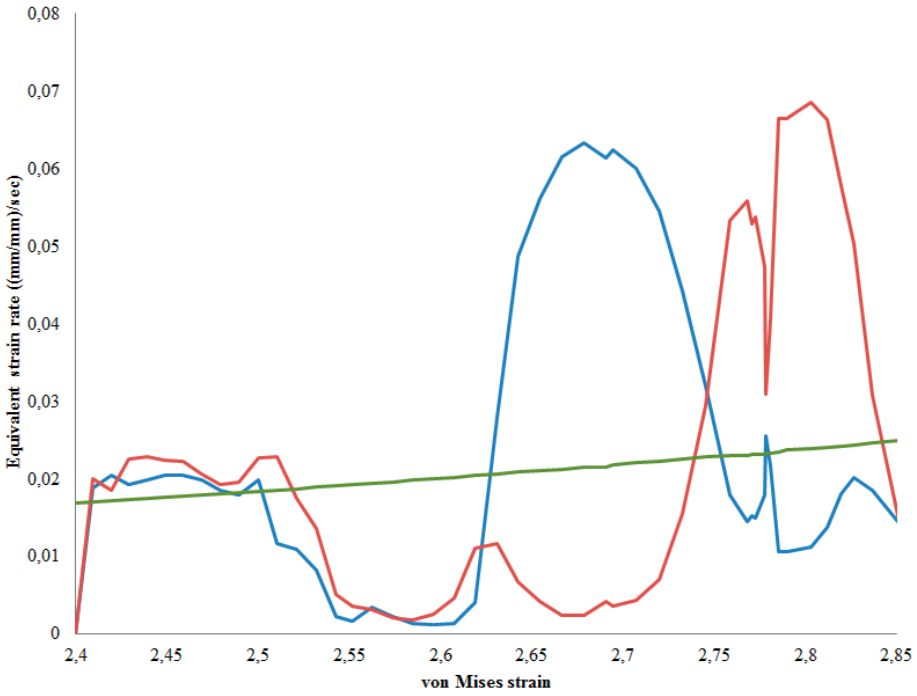

Fig.11. Variation of effective strain rate at two points located near the roll bonded interface in the AA3103 layer. The nominal strain rate based on uniform plane strain compression is shown in green.

In Fig. 11 the variation of the effective strain rate in the plane strain compression simulation shown in Figs. 9-10 is obtained by following two selected material points located in the first AA3103 layer outside the mid-layer. Before the onset of instability the strain rate of both the points coincide with the average strain rate based on the compression of the stack. Next the shear band starts to evolve and the points experience a high strain rate while being inside a shear band and a low strain rate

while being outside indicating that the shear bands are moving relatively to the Lagrangian movement of the points.

In the laminate containing many layers, the layers seem to get thinner by a collective zigzag instability. Such zigzag instabilities are extensively studied in pattern forming systems like in hydrodynamic stability theory for formation of two-dimensional roll patterns, see for example [15]. In the early onset of zigzag instability the hard layer becomes longer, and hence thinner, by increasing its length by a sinusoidal bending, as can be observed in Fig.10b. When the deformation proceeds further, this kind of instability in the layer develops and eventually causes disintegration of the hard phase. The shear band observed in the Cu layer in Fig.3 indicates the stage before disintegration of the hard layer. As can be seen from Fig. 10a the crossing shear bands have opposite sign corresponding to bending in opposite directions. Hence a material point in the hard layer is bent the one way or the other, depending on which shear band it is passing by.

4.3 FEM simulation of the 4th ARB pass of Al and Cu

The specimen with 17-layers with a continuous reinforcement of copper in aluminium was also modelled for the case of ARB to examine the instability observed during the 4th ARB pass. Symmetry across the middle of the specimen was applied, as shown in Fig. 12. Friction was defined between the rolls and the layer stack and sticking condition defined internally between the layers, and the same isotropic von Mises materials as for the plane strain compression were assumed.

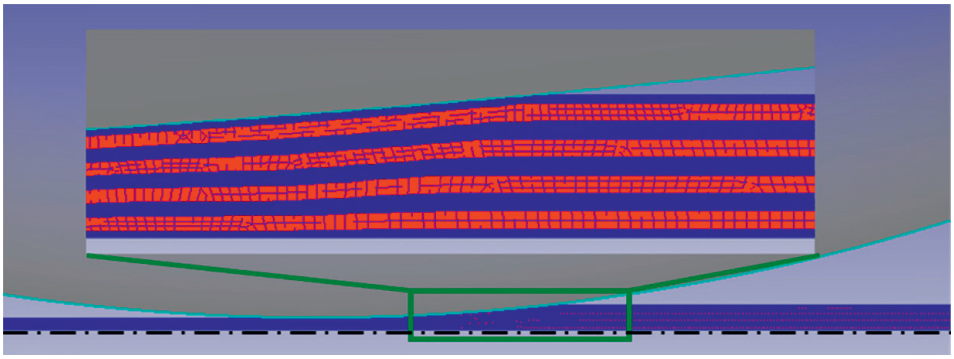

Fig.12. Multi-layer Al-Cu model used for 4th pass ARB simulations. The Al layers are shown in blue and Cu layers in red. The inset shows the layers entering the roll gap. Boundaries on the lower edge are symmetry boundaries indicating that only a half of the sample was calculated.

Figure 13 illustrates strain rate variations as the material goes through the rolling gap. The crossed shear bands are somehow similar to those of the plane strain compression simulations, but of a higher magnitude. The shear bands make a zigzag pattern cross the multilayer stack at fixed locations relative to the rolls. A material point passing through the gap between the rolls will experience bending and unbending as it passes the two opposite shear zones respectively. This causes the instability in the form of a sinusoidal two-dimensional bending of the hard layers with more pronounced shear in the soft layers. The distance between the shear bands scales with the total thickness. This scale decreases as the material passes through the gap.

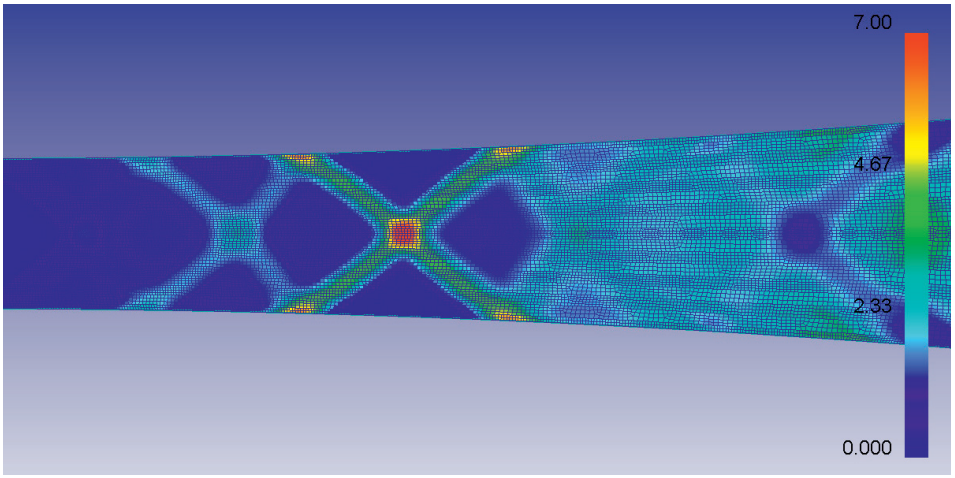

Fig.13.Strain rate plots showing alternating patterns in ARB simulation of Al and Cu multilayers deformed to a strain of around 3.

Figure 14 shows the layers after the simulation of the 4^{th} rolling pass. The instability is little developed, but an early onset is clearly identified as a bending of the layers with a wavenumber scaling with the strip thickness.

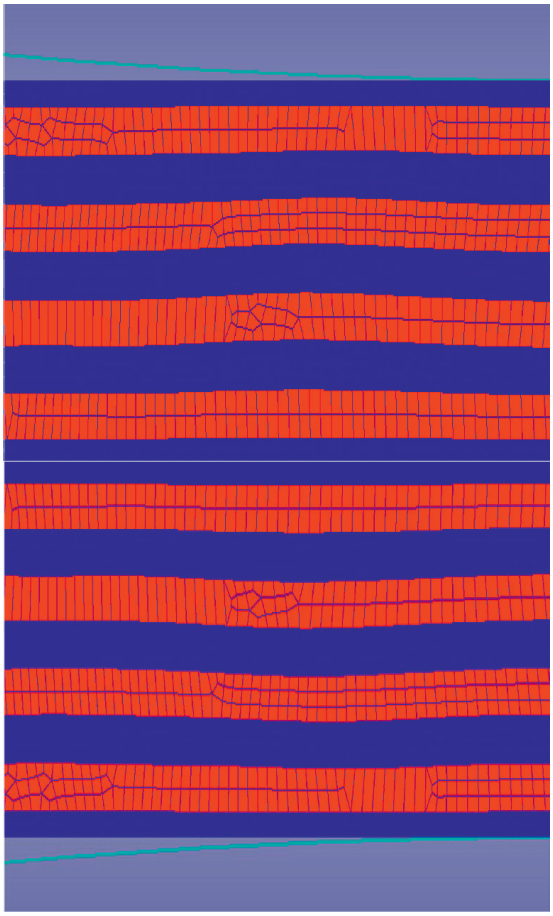

Fig.14. Simulation results showing early onset of instability in a sheet of Al and Cu multilayers at the roll gap exit subsequent to the 4th pass of ARB.

5. Discussion

The general increase in strength of the ARB specimens with increasing number of ARB cycles can be attributed to work hardening. As long as the layers do not fracture the rule of mixtures should be applicable to

predict the strength of the composites. The temperature of 350°C used for pre heating the samples before warm ARB passes is sufficient to cause significant softening in both AA3103 and Cu. Commercial pure Cu has been reported to undergo significant softening even at room temperature [16], so the strength added by work hardening is partly recovered during a subsequent warm ARB pass. However, it can be observed from Fig.4c that some hardening has also accumulated in the case of warm ARB'ed Al- Cu. The temperature acts as the controlling factor for dislocation motion and dynamic recovery with a corresponding higher strain rate sensitivity that can prevent localisation and explain the improved layer refinement during warm ARB.

In the cases of cold ARB samples, especially of Br and Al represented in Fig.4a, the strength increase is significant up to 2 passes, beyond which the samples exhibit pre-mature failure. This is most likely due to discontinuity in the hard phase due to failure. For the samples without failure, but with a discontinuous hard layer, strength levels of around 400 – 450 MPa are reached by cold ARB of Al and Br samples and 375 MPa for Al and Cu samples. These are significantly higher strengths compared to about 250 – 300 MPa obtainable by cold ARB of AA3103 without the Cu layers [17].

Although the tensile test gives a fair indication of the strength of multilayer materials, further information of the influence of layer continuity on the load bearing capacity, ductility and toughness can be obtained by the three point bend test. The general trend of the increase in the flexural strength with increasing number of ARB passes continues till the hard layers stop being continuous. When the hard layers have

disintegrated in the matrix, a drastic drop in both the flexural strength and the ductility was observed in 4 pass cold ARB of Al and Br in Fig.5a. However, the hard layer in the 5 pass cold ARB of Al and Cu does not reveal much disintegration and rupture and hence has a good flexural strength and ductility as shown in Fig.5b. This indicates that continuity of layers is the important factor determining load bearing capacity.

A distinct sequence of several load drops was observed in 2 pass cold ARB of Al and Br and 1 pass Al and Cu in Fig.5. Load drops in similar cases have been reported to correspond to the fracture and delamination of the different layers and the plateaus indicate plastic deformation of the successive layer for crack re-nucleation [18, 19]. Thus delamination in a particular layer inhibits crack propagation into the successive layer and a new crack can be nucleated only after considerable plastic deformation in the successive layer. This mechanism of interface delamination acts as an effective means of arresting cracks and delaying failure of the material as reported by Cepeda and Liu [8, 18]. However, this mechanism cannot be observed in any of the samples where the hard phase is discontinuous. Thus layer continuity seems inevitable for realizing the benefits of the multilayer material through this mechanism of interface delamination induced retardation of cracking [8]. A flexural strength as high as 750-800 MPa is exhibited by samples of cold ARB of Al and Br as long as the layers are more or less continuous, but the moment continuity is lost, the flexural strength drops to 500- 600 MPa. The low flexural strength and lacking ductility of 4 pass cold ARB of Al and Br samples can be explained similarly based on lack of layer continuity leading to early failure in the bending test.

The 45 degree shear bands cutting through the layers suggest that subsequent to the onset of instability, the thinning of the hard layers is by intersecting shear bands rather than by plane strain compression. The FEM simulations of plane strain compression showed that the onset of instability was in the form of a bifurcation from uniform plane strain compression to the formation of well-defined 45° zigzag shear bands occurring through all the layers of the strip thickness at a certain rolling reduction. The alternating shear bands will bend and unbend the layers. The zigzag instability initially makes the strong layer more elongated and hence uniformly thinner as compared to the earlier assumptions of localized necking. The distance between bending and unbending is defined by the spacing between the shear bands, which scales with the strip thickness. Since the total thickness is decreasing during compression, the bending wavelength for the layers is decreasing. In the plane strain compression case, this convectively brings new material into the shear zone and the sheared material out of it. When tracing points on the Al layer near the roll bonded interface, it was seen that before the onset of instability the strain rate corresponded to the uniform compression of the stack of layers. Subsequent to onset of instability the points experienced higher strain rates while being inside the shear band and lower strain rates while being outside, clearly defining the onset of instability in Fig. 11.

Yazar et al. [20] reported simulations of cases with a strong layer sandwiched between two thick softer layers as a prototype for investigating instability of metal laminates. They reported a similar instability as reported here, where the hard layer was intersected by shear fronts during deformation. They concluded that homogeneous refinement

of continuous structures is still possible if the reinforcement strength is not more than two times the strength of the matrix for the rigid plastic case without work hardening. In their simulation setup a sinusoidal thickness variation in the reinforcement with a wavelength equal to the thickness was necessary to destabilize the homogeneity of the deformation and generate instabilities. The simulations in Fig 9.a-d were repeated with a similar thickness variation, but showed little difference in the onset of instability, thus revealing that such thickness variation is not necessary to generate instabilities in this more realistic simulation of multilayers.

The Cu reinforcement in our case was assumed to be 50% stronger than the cold rolled AA3103 at the considered strain levels where instabilities were inevitably observed. Irrespective of the presence of thickness variations in the hard layer, deformation instabilities occur in roll bonding of dissimilar material combinations thus leading to multiple necking in the hard layer. The strain levels at which instabilities occurred in the DEFORM simulations, are comparable to the strain levels where the Cu layers exhibit significant necking in the actual ARB experiments. Also the absence of instability for the case with work hardening is consistent with the findings of Yazar et al. [20] .

The instability predicted by the 4^{th} pass ARB simulation in Fig 14 is less developed than the experimental one shown in Fig. 15. The difference can be due to the model simplifications regarding isotropic material, two-dimensionality, stiffness of the rolls and friction conditions. The ratio of the yield stresses of the two materials after three passes might have been

estimated slightly too low, which will delay the onset of instability according to Yazar et al. [20].

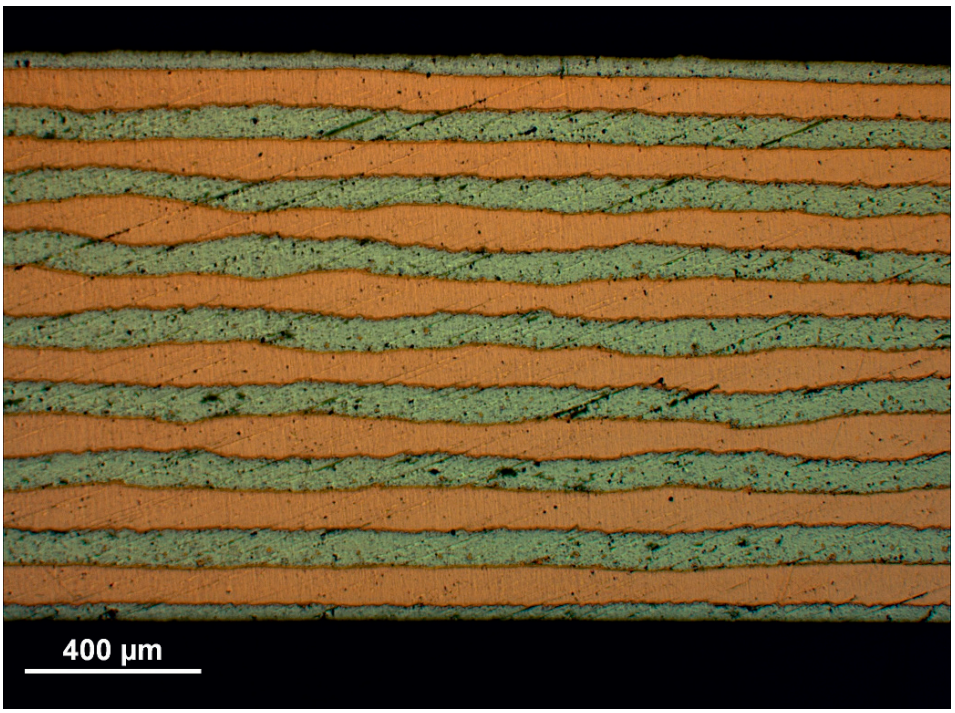

Fig.15.Optical micrograph showing early onset of instability in a sheet of Al and Cu multilayers subsequent to the 4^{th} pass of ARB.

Layer continuity is very important to realize the beneficial effects of multi-layer composites. Experiments and simulations however indicate that the hard layer is bound to disintegrate owing to the zigzag instability caused by the difference in flow properties with the soft layer. This effect, although difficult to eliminate, can be delayed by careful selection and control of the strength ratio between the layers. This can be altered

by heat treatments and by warm roll bonding instead of cold roll bonding. However, warm conditions may cause formation of intermetallic phases at the interfaces between the metals. Higher temperature is indeed found to give a better control of the layer thickness in the considered experimental work and work hardening of the hard layer was sufficient to avoid instability in the simulations. Ductility and toughness also get affected and annealing steps are unavoidable at some stage.

6. Conclusions

Cold ARB of multilayer metal composites were successfully performed up to 17 layers by 4 passes of Al and Br and up to 33 layers with 5 passes of Al and Cu in alternating layers. Further passes of cold ARB were prevented by severe flow instabilities with disintegration of the hard layers and cracking of the composite. ARB of Al and Cu layers at 350°C up to 6 passes resulted in multilayer metal composites with 64 Al and Cu layers. Only a weak onset of instability of the strong layer could be observed in this case, but further ARB was not possible due to severe edge cracking. Estimates about the onset of instability from simplified analytical solutions were found not to apply as the simplifying assumptions are considered not to be realistic. The observed instability mode was two-dimensional and two-dimensional FEM simulations were performed. The predicted onset and mode of instability were in good agreement with what was found for the cold ARB of Al and Cu. The simulations showed that the instability mode is a zigzag-shear instability, where crossing 45° shear bands form and the result is a sinusoidal type of bending of the strongest layer by the opposite crossing shear bands. The

earlier assumption of localization due to periodic localized necking is not confirmed. Instead a zigzag pattern of shear bands forms as a bifurcation of the uniform plane strain compression mode at onset of instability. Initially these shear bands makes the layers more elongated and hence uniformly thinner. The onset of instability seems to correlate with the end of stage IV work hardening, a stage where there is lack of further work hardening of the strong layer. Layer control to avoid or extend this type of instability, might be possible by careful selection and control of the strength ratio and work hardening of the involved metal layers. FEM simulations are a valuable tool for predicting this type of instability.

REFERENCES

[1] Eizadjou M, Kazemi Talachi A, Danesh Manesh H, Shakur Shahabi H, Janghorban K. Investigation of structure and mechanical properties of multi-layered Al/Cu composite produced by accumulative roll bonding (ARB) process. Composites Science and Technology. 2008;68:2003-9.

[2] McKeown J, Misra A, Kung H, Hoagland RG, Nastasi M. Microstructures and strength of nanoscale Cu-Ag multilayers. Scripta Materialia. 2002;46:593-8.

[3] Srivastava A, Yu-Zhang K, Kilian L, Frig, rio J, Rivory J. Interfacial diffusion effect on phase transitions in Al/Mn multilayered thin films. Journal of Materials Science. 2007;42:185-90.

[4] Chen MC, Hsieh HC, Wu W. The evolution of microstructures and mechanical properties during accumulative roll bonding of Al/Mg composite. Journal of Alloys and Compounds. 2006;416:169-72.

[5] Min G, Lee J-M, Kang S-B, Kim H-W. Evolution of microstructure for multilayered Al/Ni composites by accumulative roll bonding process. Materials Letters. 2006;60:3255-9.

[6] Hebert RJ, Perepezko JH. Deformation-induced synthesis and structural transformations of metallic multilayers. Scripta Materialia. 2004;50:807-12.
[7] Lee J-M, Lee B-R, Kang S-B. Control of layer continuity in metallic multilayers produced by deformation synthesis method. Materials Science and Engineering: A. 2005;406:95-101.
[8] Liu HS, Zhang B, Zhang GP. Enhanced toughness and fatigue strength of cold roll bonded Cu/Cu laminated composites with mechanical contrast. Scripta Materialia. 2011;65:891-4.
[9] Atkins AG, Weinstein AS. The deformation of sandwich materials. International Journal of Mechanical Sciences. 1970;12:641-57.
[10] Bourdeaux F, Yavari R. Multiple necking and deformation behaviour of multilayer composites prepared by cold rolling. Z Metallkde. 1990;81:130.
[11] Hwang Y-M, Hsu H-H, Lee H-J. Analysis of plastic instability during sandwich sheet rolling. International Journal of Machine Tools and Manufacture. 1996;36:47-62.
[12] Nowicke Jr F, Zavaliangos A, Rogers HC. The effect of roll and clad sheet geometry on the necking instability during rolling of clad sheet metals. International Journal of Mechanical Sciences. 2006;48:868-77.
[13] Semiatin SL, Piehler HR. Formability of sandwich sheet materials in plane strain compression and rolling. Metallurgical Transactions A. 1979;10:97-107.
[14] Steif PS. On deformation instabilities in clad metals subjected to rolling. Journal of Applied Metalworking. 1987;4:317-26.
[15] Holmedal B, Tveitereid M, Palm E. Planform selection in Rayleigh–Bénard convection between finite slabs. Journal of Fluid Mechanics. 2005;537:255-70.
[16] Kuo C-M, Lin C-S. Static recovery activation energy of pure copper at room temperature. Scripta Materialia. 2007;57:667-70.
[17] Haaland BØ, Westermann I, Holmedal B, Nes EA. Microstructure and properties of as-deformed and annealed accumulated roll-bonded aluminium alloys. In: Hirsch J, Gottstein G, Skrotzki B, editors. 11'th International

conference on aluminium alloys. Aachen, Germany: Wiley-VCH; 2008. p. 1468-73.
[18] Cepeda-Jiménez CM, Pozuelo M, García-Infanta JM, Ruano OA, Carreño F. Interface Effects on the Fracture Mechanism of a High-Toughness Aluminum-Composite Laminate. Metallurgical and Materials Transactions A. 2009;40:69-79.
[19] Cepeda-Jiménez CM, Alderliesten RC, Ruano OA, Carreño F. Damage tolerance assessment by bend and shear tests of two multilayer composites: Glass fibre reinforced metal laminate and aluminium roll-bonded laminate. Composites Science and Technology. 2009;69:343-8.
[20] Yazar Ö, Ediz T, Öztürk T. Control of macrostructure in deformation processing of metal/metal laminates. Acta Materialia. 2005;53:375-81.

ACKNOWLEDGEMENTS

The present study was financed by the Norwegian Research Council under the Improvement project of the Strategic University Program (192450/I30).